Crystal Structure and Bonding in Transition-Metal Fluoro Compounds

WERNER MASSA and DIETRICH BABEL*

Fachbereich Chemie der Philipps-Universität, D3550 Marburg, Federal Republic of Germany

Received April 13, 1987 (Revised Manuscript Received September 21, 1987)

Contents

I. Introduction

The most electronegative element, fluorine, gives rise to the most ionic ligands. Such ligands are among the smallest and most rigid. These features make the crystal structures of metal fluorides comparatively simple and mainly governed by geometric and electrostatic principles. This class of compounds is therefore well suited for checking the usefulness and the limits of, for example, rigid-sphere concepts (in which radius ratios predetermine coordination numbers) and at the same time the validity of Pauling's rules, which postulate local balance of charges.[1,2]

In addition to collective properties, such as size and charge, the ions have individual properties, mainly determined by their electronic configuration. Transition-metal ions in particular are expected to affect the crystal structures of their compounds through a variety of electronic effects, such as covalency, back-bonding, spin state, or generally ligand field splitting, and—most dramatically—Jahn–Teller distortion. The better we know to what degree purely geometric and electrostatic principles predetermine crystal structures, the more admissible it becomes to interpret deviations from these expectations as being caused by bonding and electronic effects (which generally only modify the basic structural patterns).

To demonstrate the structural influence of the factors mentioned we will concentrate on 3d transition-metal fluorides. Most of the structure types occurring in this class of compounds will be tabulated, provided they have been determined by X-ray single-crystal work; no attempt will be made to specify the huge variety of isomorphs reported to date. Instead, examples will be selected to illustrate certain principles of structure and bonding. Most of these concern polynary compounds, including some hydrates for the study of hydrogen bridge effects.

The literature is covered up to 1986, which was the centenary year of the isolation of fluorine by Moissan. On that occasion a special report appeared on the first 100 years of fluorine chemistry; the reader is referred to it for the many interesting aspects of the chemistry of this element.[3] More especially, in the field of chemistry and physics of inorganic solid fluorides, a recent publication edited by Hagenmuller[4] will provide the information on such important topics as preparative methods, high oxidation states, or physical properties, all of which are absent in the present article. Structural reviews giving more details also exist, including those on lanthanide and actinide fluorides.[5–10]

II. Coordination Behavior in Fluoride Structures

A. Coordination around "Central" Cations

In most oxidation states of d transition-metal ions M, the radius ratio $r_M:r_F$ falls within the range 0.41–0.73, i.e., just the stability field of octahedral coordination. This coordination is in fact observed in the majority of cases and it is quite unaffected by the F:M stoichiometry of the compound. Exceptions involve cations with the d^8 and even d^9 electronic configurations, especially those of the heavier elements, which in fluorides, too, often show the square-planar coordination usually

0009-2665/88/0788-0275$06.50/0

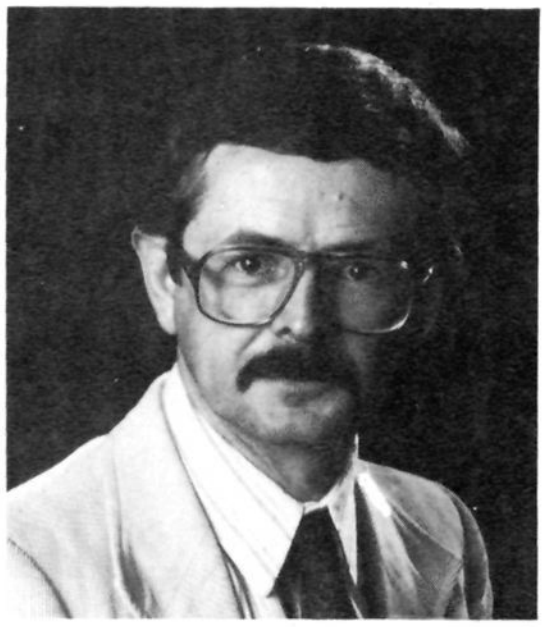

Werner Massa was born in 1944 and grew up in Riedlingen, Germany. He received his Dipl. Chem. (1969) and doctoral degrees (1972) at the University of Tübingen, where he worked in the group of Professor W. Rüdorff. In 1977 he joined the laboratory of Professor D. Babel at the University of Marburg. Since 1979 he has been directing the laboratory of X-ray crystal structure determination of the Fachbereich Chemie. After his Habilitation in 1982 he was appointed Privatdozent at the University of Marburg, where he currently is teaching. His research interests are structural chemistry, magnetism, and hydrogen bonding in inorganic solid fluorides of transition metals, especially of the Jahn–Teller active ion Mn(III).

Dietrich Babel was born 1930 in Bonn, Germany, and received his Dipl. Chem. (1958) and Dr. rer. nat. (1961) degrees at the University of Tübingen, where he was advised by Professor W. Rüdorff. After spending one term (1961/1962) with Professor W. Hoppe in Munich, to get acquainted with the techniques of X-ray single-crystal structure determination, he went back to Tübingen. He completed his Habilitation (1968) there, became a staff member (1969) in the Department of Inorganic Structural Chemistry in Tübingen, and then got a call (1970) to a chair of Inorganic Chemistry at the Philipps-University of Marburg, where he was appointed Professor (1971). He was a member of the Sonderforschungsbereich 127 "Crystal Structure and Chemical Bonding" (1974–1986) and during two periods (1977/1978 and 1986/1987) dean of the Fachbereich Chemie in Marburg. For a sabbatical leave (1981) he was absent one term for Bordeaux, at Professor P. Hagenmuller's Institute. His research interests are in the general area of solid-state chemistry, with special emphasis on crystal structure systematics and magnetochemistry, investigated mostly at transition-metal fluorides and cyanides.

found for these configurations.[10–16] On the other hand, there are rare cases of tetrahedral 4-coordination, e.g., in the scheelite type structure of $CaZnF_4$.[17] In fact, zinc is a central cation with a well-known preference for tetrahedral sites.

TABLE I. Fluoride Crystal Structures Containing Isolated [MF_6]octahedra

	prototype	CN of A ion	space group	Z	ref
AMF_6	$LiSbF_6$	Li: 6	$R\bar{3}$	1	19
	$NaSbF_6$	Na: 6	$Fm3m$	4	20
	$KNbF_6$	K: 8	$P\bar{4}c2$	2	21, 22
	$KOsF_6$	K: 12	$R\bar{3}$	1	23, 24
	$BaSiF_6$	Ba: 12	$R\bar{3}m$	1	24–26
A_2MF_6	Li_2ZrF_6	Li: 6	$P\bar{3}1m$	1	27, 28
	Na_2SiF_6	Na: 6	$P321$	3	29, 30
	Na_2SnF_6	Na: 6	$P2_1/c$	2	28, 31
	K_2GeF_6	K: 12	$P\bar{3}m1$	1	32
	K_2MnF_6	K: 12	$P6_3mc$	2	33
	K_2SiF_6	K: 12	$Fm3m$	4	34
	$CaLiAlF_6$	Ca: 6, Li: 6	$P\bar{3}1c$	2	35
	$SrLiFeF_6$	Sr: 6+2, Li: 6	$P2_1/c$	4	36
	$BaLiCrF_6$	Ba: 12, Li: 4	$P2_1/c$	4	37
A_3MF_6	α-Li_3AlF_6	Li: 6	$Pna2_1$	4	38
	β-Li_3VF_6	Li: 6 and 4	$C2/c$	12	39
	Na_3AlF_6	Na: 6+6 and 6	$P2_1/n$	2	40–42
	Rb_3TlF_6	Rb: 10 and 8	$I4/mmm$	2	43
	K_3MoF_6	K: 12 and 6	$Fm3m$	4	44
	Hg_3NbF_6	Hg chains	$I4_1/amd$	4	45
		Hg layers	$P\bar{3}1m$	1	46
	$Na_3Li_3Al_2F_{12}$	Na: 8, Li: 4	$Ia3d$	8	47, 48
	K_2NaAlF_6	K: 12, Na: 6	$Fm3m$	4	49–51
	K_2LiAlF_6	K: 12, Li: 6	$P3m1$	3	52, 53
	Cs_2NaCrF_6	Cs: 12, Na: 6	$R\bar{3}m$	6	54–56
	Cs_2LiGaF_6	Cs: 12, Li: 6	$P\bar{3}m1$	1	54
A_2MF_7	Ca_2AlF_7	Ca: 7 and 7+1	$Pnma$	4	57
	Pb_2RhF_7	Pb: 7+2 and 8+2	$P2_1/c$	4	58
	$BaCaCrF_7$	Ba: 12, Ca: 8	$P2/n$	4	59

While the number of transition-metal fluorides exhibiting coordination numbers (CN) smaller than 6 is quite limited, coordination numbers *higher* than 6 are more frequent. They occur with the larger cations, which in addition to some d elements as zirconium and hafnium typically comprise the f-series elements of the lanthanides and actinides. However, neither the structures found for the fluorides of these elements[7,8] nor others with CN $\neq$ 6 will be dealt with in this paper.

When dealing with the d transition-metal fluorides, we shall pay less attention to the well-known structures of binary compounds MF_n (n = 2–6)[9] and to those derived from the latter by substitution of differently charged cations, e.g., trirutiles like $LiM^{II}M^{III}F_6$ or VF_3- and ReO_3-type related structures like $LiSbF_6$ and $NaSbF_6$, respectively. Though a large number of compounds adopting these (pseudo)binary structures are known,[10] the structural variety in this class is rather limited. This is even more true of the structures of the alkali-metal and alkaline-earth fluorides AF and AF_2, respectively, the most common binary components of ternary transition-metal fluorides A_mMF_n. The simplest illustration of structural monotony in binary fluorides is the rock salt structure adopted by all the alkali-metal fluorides AF, regardless of the broad radius ratio range, which varies from r_A/r_F = 0.57 in LiF to 1.26 in CsF. This demonstrates the constraints imposed by stoichiometry, i.e., the composition of a compound, which is the most important of the factors influencing the geometry of a structure. Even the relative-size effect is controlled by the composition, which provides the number and proportion of building units to set up a structure.

B. Countercations in Polynary Fluorides

When going from binary to ternary compounds A_mMF_n, both cations, A and M, have access to more

fluoride anions than before and therefore get a better chance to display differences in their coordination behavior according to their radius ratios r_A/r_F and r_M/r_F. As already mentioned, the result is nearly invariably octahedral coordination for the d transition-metal ions, which form negatively charged $[MF_6]$ units, isolated or linked (see later). The remaining positive elements A then play the role of countercations and influence the arrangement of these units in such a way as to achieve an optimum AF_n coordination. The resulting CNs of alkali-metal ions observed in a vast variety of polynary fluorides—unlike the constant CN 6 in the binary alkali-metal fluorides—are well differentiated and clearly follow the radius ratio r_A/r_F given for the element. The larger ions, K^+, Rb^+, and Cs^+, tend to close-pack with the similarly sized fluoride ion and therefore prefer CN 12. With only a few exceptions they exhibit at least 8-coordination. The smallest alkali-metal ion, Li^+, on the other hand, is generally only 6- or even 4-coordinated in polynary fluorides. In most fluoride compounds the sodium ion, Na^+, exhibits CNs between 6 and 8, consistent with its intermediate size. A similar gradation is observed for the alkaline-earth ions from Mg^{2+} (CN 6) to Ba^{2+} (CN 12). In Table I the CN of the countercations is shown for illustration.

III. Geometrical Features of Octahedrally Coordinated Fluoro Compounds

A. Isolated $[MF_6]$ Groups

Table I contains the most important structures reported for ternary and quaternary fluorides exhibiting isolated $[MF_6]^{m-}$ octahedra. These are generally formed if the stoichiometric ratio F:M ≥ 6, except for M in oxidation state +2.[18]

1. The Group of Cryolites and Elpasolites

As in most ternary compounds of general composition A_mMF_6, isolated octahedral $[MF_6]$ groups are also present in the "cryolites" A_3MF_6 and more especially in the "elpasolites" A_2BMF_6, named after the mineral K_2NaAlF_6.[49] This group of compounds is chosen here to show the size effect of the constituent ions ($r_A > r_B > r_M$) on the resulting structure.

When the two alkali-metal ions are different, A and B, the cryolite structure becomes cubic. This is generally not the case if they are both the same. The true cryolites Na_3MF_6 are monoclinic.[40-42] Most of the corresponding compounds with the larger alkali-metal ions have complicated superstructures of varying complexity, the majority of which have not yet been solved.[60,61]

The reason why (with some exceptions, especially involving high-temperature phases) only the elpasolites A_2BMF_6 adopt the idealized cubic cryolite structure is obviously purely geometric: the size difference between the large (A) and the small (B) ions matches the difference between the 12- and 6-coordinated cavities provided by the cubic structure shown in Figure 1.

The geometric conditions for the appearance of cubic symmetry and the relations between ionic radii and lattice constants in elpasolites are discussed in the following.

a. The Tolerance Factor and Its Geometrical Meaning. The elpasolite structure is a perovskite superstructure with doubled cell edge. It results from substitution of the two M^{II} cations in $A^I_2M^{II}M^{II}F_6$ by two unlike ions $B^I + M^{III}$, which order, because of differences in charge and size, on the octahedral sites in $A^I_2B^IM^{III}F_6$. The radius ratio relation for the perovskites, known as the Goldschmidt tolerance factor,[62] is therefore also applicable to the elpasolites. It turns out that elpasolites are cubic if their tolerance factor $t = 2^{1/2}(r_A + r_F)/(r_M + r_B + 2r_F)$ lies within the limits $0.88 \leq t \leq 1.00$.[10,63] The upper limit, $t = 1$, means that all cations are in contact with anions. As a result, in both rows of ions, that along the cell edge ($r_M + r_B + 2r_F = a_e/2$) and the other along the cell diagonal (projected on the edge: $2^{1/2}(r_A + r_F) = a_d/2$), the radii add up to the same value, which should be identical with the observed lattice constant, $a_0 = a_e = a_d$. However, the cubic structure tolerates loss of diagonal contact, as shown by the lower limit of $t = a_d/a_e = 0.88$.

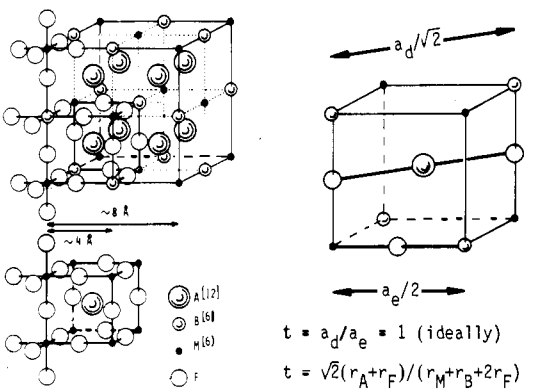

Figure 1. Structure of cubic elpasolites A_2BMF_6 as related to AMF_3 perovskites and the geometrical meaning of Goldschmidt's tolerance factor t.

In practice, it is often found, especially for compounds in the lower tolerance factor range, that the observed lattice constants are smaller than calculated from the edge-row ionic radii, $a_0 < a_e$. In fact single-crystal structure analyses and spectroscopic studies provide evidence of anion displacements from the ideal positions on the cell edges, such displacements accounting for some contraction.[51] However, if these details are disregarded, another idea, well-known from Vegard's rule,[2] may be applied to account for a variation of lattice constants: Since the cell dimensions of solid solutions are generally determined from those of the constituents according to their proportion, the lattice constants of the elpasolites should depend on the atom dimensions both along the edge and along the diagonal.

b. Ionic Radii and Lattice Constants of Elpasolites. The foregoing assumption leads to the simple expression $a = (a_d + a_e)/2$. For example, with the above definitions, and using the well-accepted Shannon radii[64] for the appropriate CNs and $r_F = 128.5$ pm, for Rb_2KFeF_6 ($t = 0.89$) $a_d = 849.9$ and $a_e = 919.0$ pm yield $a = 884.5$ pm, compared to the observed lattice constant $a_0 = 886.7$ pm (powder work) and 886.9 pm (single crystal).[51,63] In other words, the mean value of the diagonal and the edge radii sums, the ratio of which is the tolerance factor, gives a better approximation to the observed constant than either component alone.

Explicitly, this expression for predicting the cubic elpasolite lattice constants becomes $a = 2^{1/2}r_A + r_B + r_M + (2 + 2^{1/2})r_F$, which is a linear combination of ionic

radii with special coefficients. Generalizing the expression to

$$f_A r_A + f_B r_B + f_M r_M + f_F r_F = a_c$$

it should be possible to calculate better lattice constants a_c, provided the coefficients f_i can be properly adjusted from a suitable selection of compounds. Conversely, this relation may be used to determine ionic radii. Table II gives the results for 81 elpasolites A_2BMF_6 (65 only with experimental a_0) and a set of optimum radii for the 18 cations, 4 of type A (CN 12), 5 of type B (CN 6), and 9 of type M (CN 6). In separating the products $f_i r_i$ the radii were chosen as close as possible to the Shannon values and r_F was fixed to 128.5 pm.

Since the observed lattice constants a_0, which are the basis of this evaluation of ionic radii and their coefficients, $f_i r_i$, are subject to experimental error, they have to be balanced before use. A method to do this at isostructural compounds has been given by Waddington.[65] The result is equivalent to a least-squares refinement and yields balanced values $a_c = \bar{a}_I + \bar{a}_{III} - \bar{a}$. These are calculated from the observed average constants $\bar{a}_I$ of all compounds A_2BMF_6 with the same cations A_2B, the average constants $\bar{a}_{III}$ of the compounds with the same M cation, and finally the overall average lattice constant $\bar{a} = \sum a_0/mn$ of the mn compounds used in a full matrix. As only 65 a_0 values were available at the time of writing for the $9 \times 9 = 81$ compounds listed in Table II, roughly calculated values were used for the remaining 16 compounds instead of a_0. These are the figures given in parentheses.

The set of balanced lattice constants a_c obtained in this way is reproduced with the following coefficients:

$$a_c = 1.289 r_A + 1.104 r_B + 1.518 r_M + 3.222 r_F$$

The deviation of the coefficients from the special values $2^{1/2}$, 1, and $(2 + 2^{1/2})$, respectively, reflects the differing effect of the cations. This effect increases with decreasing CN and increasing charge. The above expression refers to the adapated radii r_c introduced at the same time and also given in Table II. The Shannon figures are noted for comparison. The maximum deviation of both radii sets exceeds 3% only in the case of Mo(III).[66]

As is obvious from the a_0/a_c ratios of Table II, the agreement between the observed and the calculated lattice constants is still better: 0.5% in the worst case and 0.1% on the average. Thus the figures differ hardly more than the spread in the reported lattice constants. A similar agreement between observed and calculated cell dimensions has recently been achieved for the pyrochlores $CsM^{II}M^{III}F_6$.[67]

If the tolerance factors t_c are calculated on the basis of the adapted radii r_c of Table II, using Shannon's fluoride ionic radius $r_F = 128.5$ pm for CN 2 (which reproduces best the M–F distances known from complete structure determinations), the cubic compounds listed cover the range $0.91 \leq t_c \leq 1.06$. In this form the figures express the 15% tolerance, −9% and +6%, respectively, in the radii sums along the diagonal and the cell edge that still produces a cubic elpasolite structure. A similar size range is known to limit isomorphous replacement in solid solutions.[2] Obviously, the same regularities, including Vegard's rule, also apply to the more special case of compounds if these, like the elpasolites, are subject to the geometric requirements of more than one species and are forced to find a compromise between them.

Tl_2NaTiF_6[74] happens to be an example with $t_c = 1$ in which both dimensions, a_d and a_e, are the same and equal to the observed lattice constant a_0. In Table II, however, corrected values $t = 0.956 t_c$ are given to achieve optimum agreement with tolerance factors previously published[10,63] and based on the Shannon radii for CN 6, with only r_A enlarged by a factor of 1.06. In that case the upper limit for the cubic range becomes $t = 1$. The only compound in Table II exceeding this limit slightly is K_2LiAlF_6, which is known to be polymorphic.[52,53]

c. Cubic High-Pressure Polymorphs of Elpasolites. In general, elpasolites exceeding $t = 1$ display hexagonal structures. Several types are known, depending on t and differing in the sequence of close-packed AF_3 layers.[10,54-56] At high pressure they transform to the cubic structure, in which the packing is simply ABC. As discussed elsewhere,[10,77] these transformations, which proceed stepwise and lead to metastable polymorphs, may be rationalized by arguments involving variations of the tolerance factor induced by high pressure. The ions and distances A–F being more compressible than those of B–F and M–F, they make the tolerance factor decrease under pressure and reach the cubic range this way. Release of pressure should then lead to larger B–F and M–F distances in the metastable cubic phases than are observed in the normal-pressure modifications. This expansion, caused by A ions normally too large for the cubic cage, has in fact been found by structure determinations in both polymorphs in the case of Rb_2LiFeF_6 and Cs_2NaFeF_6.[78] Another test may be performed by applying the above radii/lattice constant relation to cubic high-pressure forms of the elpasolites A_2BMF_6.

Table III lists the corresponding compounds known to date[77] along with the items as for the normal-pressure cubic elpasolites (given in Table II). For the high-pressure phases, all the calculated lattice constants a_c turn out to deviate considerably from those observed, a_0. The average deviation of about 1% is 10 times larger than in the normal-pressure phases and always corresponds to $a_0 > a_c$. This is in accordance with the expansion predicted for the pressure-released metastable phases and demonstrates the applicability of the simple geometric model which underlies the tolerance factor concept.

The above relation may also be used to calculate ionic radii, especially those for the less usual M^{III} oxidation states stabilized in cubic elpasolites. Applied to Cs_2KCuF_6 ($a_0 = 889.4$ pm)[79] a radius $r_{Cu} = 54.7$ pm results, close to the low-spin value of Cu^{III} given by Shannon (54 pm).[64]

B. M–F–M Bridges between [MF_6] Groups

Ligands bridging metallic centers are the links generally between polyhedra. How polyhedra are connected to form networks has been systematically treated by many authors in reviews and even textbooks.[2] These systematics have been applied mostly to oxides, among which the silicates[79a] provide well-described examples of tetrahedral and other minerals[79b] of mixed tetrahedral/octahedral networks. The following discussion

TABLE II. Lattice Constants (pm) as Observed (a_0) and Calculated (a_c) for Cubic Elpasolites A_2BMF_6[a,b]

		M[a]																	
		Al[c] 53.5 (53.5)		Ga[d] 61.2 (62.0)		Co[e] 61.2 (61)		Cr[f] 61.3 (61.5)		Fe[g] 64.5 (64.5)		V[h] 64.9 (64.0)		Rh[i] 65.9 (66.5)		Ti[j] 69.1 (67.0)		Mo[k] 74.8 (69)		
A_2B[a]	r_c ($r_{Shannon}$)																			$\bar{a}_I$
K_2Li	161.0 (164)	786.5[i]	1.014[iii]	798.0	0.994	799.5	0.994	798.0	0.994	802.0	0.986	802.0	0.985	(804.8)	0.982	809.4	0.975	(818.0)	0.961	802.02
	75.5 (76)	786.0[ii]	1.001[iv]	797.7	1.000	797.7	1.002	797.8	1.000	802.7	0.999	803.3	0.998	804.9	1.000	809.7	1.000	818.3	1.000	
Tl_2Na	174.7 (170)	837.0	0.994	845.3	0.976	(846.4)	0.976	846.6	0.975	850.1	0.968	850.9	0.967	852.6	0.965	856.6	0.958	864.9	0.945	850.04
	102.0 (102)	833.0	1.005	844.7	1.001	844.7	1.002	844.8	1.002	849.7	1.000	850.3	1.001	851.9	1.001	856.7	1.000	865.3	1.000	
Rb_2Na	173.1 (172)	829.8	0.989	840.6	0.970	841.9	0.970	842.0	0.970	846.5	0.963	847.0	0.962	849.2	0.960	853.3	0.952	863.2	0.940	845.94
	102.0 (102)	830.9	0.999	842.6	0.998	842.6	0.999	842.7	0.999	847.6	0.999	848.2	0.999	849.8	0.999	854.6	0.998	863.2	1.000	
Cs_2K	188.0 (188)	888.1	0.959	(899.3)	0.942	899.8	0.942	899.0	0.942	904.6	0.936	904.4	0.935	904.9	0.933	911.2	0.926	921.0	0.915	903.59
	135.9 (138)	887.5	1.001	899.2	1.000	899.2	1.001	899.3	1.000	904.2	1.000	904.8	1.000	906.4	0.998	911.2	1.000	919.8	1.001	
K_2Na	161.0 (164)	812.2	0.949	826.6	0.931	826.0	0.931	827.5	0.931	832.1	0.924	831.5	0.923	836.2	0.921	839.8	0.914	850.1	0.902	831.33
	102.0 (102)	815.3	0.996	827.0	1.000	827.0	0.999	827.1	1.000	832.0	1.000	832.6	0.999	834.2	1.002	839.0	1.001	847.6	1.003	
Cs_2Rb	188.0 (188)	905.1	0.927	(916.3)	0.912	913.5	0.912	915.0	0.912	920.2	0.906	923.9	0.905	(923.5)	0.903	(928.3)	0.897	(936.9)	0.886	920.30
	151.0 (152)	904.2	1.001	915.9	1.000	915.9	0.997	916.0	0.999	920.9	0.999	921.5	1.003	923.1	1.000	927.9	1.000	936.5	1.000	
Cs_2Tl	188.0 (188)	907.0	0.924	918.2	0.909	(917.5)	0.909	916.6	0.909	922.2	0.903	923.3	0.902	(924.8)	0.900	(929.6)	0.894	939.3	0.883	922.06
	152.6 (150)	906.0	1.001	917.7	1.001	917.7	1.000	917.8	0.999	922.7	0.999	923.3	1.000	924.9	1.000	929.7	1.000	938.3	1.001	
Tl_2K	174.7 (170)	867.9	0.918	881.8	0.903	(881.6)	0.903	882.4	0.903	888.0	0.896	887.1	0.895	(888.8)	0.893	(893.6)	0.887	897.7	0.876	885.43
	135.9 (138)	870.4	0.997	882.1	1.000	882.1	0.999	882.2	1.000	887.1	1.001	887.7	0.999	889.3	0.999	894.1	0.999	902.7	0.994	
Rb_2K	173.1 (172)	868.2	0.913	(881.1)	0.898	881.0	0.898	880.9	0.898	886.7	0.891	887.5	0.891	887.6	0.889	893.8	0.883	(901.7)	0.872	885.39
	135.9 (138)	868.3	1.000	880.0	1.001	880.0	1.001	880.1	1.001	885.0	1.002	885.6	1.002	887.2	1.000	892.0	1.002	900.6	1.001	
	$\bar{a}_{III}$	855.76		867.47		867.47		867.56		872.49		873.07		874.71		879.51		888.09		871.79[l]

[a] For each M–A_2B combination the data are tabulated as follows: (i) a_0, (ii) a_c, (iii) t, (iv) a_0/a_c. $\bar{a}_I$, $\bar{a}_{III}$, and $\bar{a}$ are the mean values used to derive a balanced set (see text): $a_c = \bar{a}_I + \bar{a}_{III} - \bar{a} = 1.289r_A + 1.104r_B + 1.518r_M + 3.222r_F$. The tolerance factor $t = 0.956t_c$, based on $t_c = 2^{1/2}(r_A + r_F)/(r_B + r_M + 2r_F)$ using $r_F = 128.5$ pm and adapted radii r_c as in the expression above and listed for the cations A, B, and M. [b] See ref 10. [c] Reference 68. [d] Reference 63. [e] References 63 and 69. [f] References 63 and 70. [g] References 63 and 71. [h] References 63 and 72. [i] Reference 73. [j] References 74 and 75. [k] Reference 76. [l] $\bar{a}$.

TABLE III. Observed (a_0) and Calculated (a_c) Lattice Constants (pm) of Cubic High-Pressure Modifications of A_2BMF_6 Elpasolites[a,b]

		M[a]									
		Al 53.5		Ga 61.2		Cr 61.3		Fe 64.5		V 64.9	
A_2B[a]	r_c										
Tl_2LiMF_6	174.7	—[i]	1.062[iii]	820.8	1.041	—	1.041	832.9	1.003	—	1.032
	75.5	803.8[ii]	—[iv]	815.4	1.007	815.6	—	820.5	1.015	821.1	
Rb_2LiMF_6	173.1	—	1.056	—	1.036	—	1.035	824.4	1.027	824.8	1.026
	75.5	801.7	—	813.4	—	813.5	—	818.4	1.007	819.0	1.007
Cs_2NaMF_6	188.0	862.8	1.037	—	1.018	870.6	1.018	873.9	1.010	875.2	1.009
	102.0	850.2	1.015	861.8	—	862.0	1.010	866.9	1.008	867.5	1.009

[a] For each M–A_2B combination the data are tabulated as follows: (i) a_0, (ii) a_c, (iii) t, (iv) a_0/a_c. Tolerance factor $t = 0.956t_c$, based on $t_c = 2^{1/2}(r_A + r_F)/(r_B + r_M + 2r_F)$ using $r_F = 128.5$ pm and adapted radii r_c as listed for the cations A, B, and M. [b] Reference 77.

TABLE IV. Fluoride Structure Types Displaying Single Bridges (Corner-Sharing Only)[a]

Chain Structures

single chain			double chain		triple chain	
type	cis bridged	trans bridged	type		type	
$A^I_2MF_5$	K_2FeF_5 (80)	"Tl_2AlF_5" (89, 90)	$A^IA^{II}M^{III}_2F_9$	$KPbCr_2F_9$ (108)	A^IMF_4	$KCrF_4$ (112, 113)
	Rb_2CrF_5 (81, 82)	$A_2AlF_5 \cdot H_2O$ (90–92)		$NaBaFe_2F_9$ (109)		$CsCrF_4$ (114–116)
		A_2MnF_5 (93–97)				
		$A_2MnF_5 \cdot H_2O$ (98–100)				
$A^{II}MF_5$	$SrFeF_5$ (83)	$CaCrF_5$ (101–104)	$A^{II}_2M^{II}M^{III}F_9$	Ba_2ZnAlF_9 (110)	ring	
		$CaFeF_5$ (105)				
	$BaGaF_5$ (84–87)	$BaFeF_5$ (103, 106)		Ba_2CoFeF_9 (111)	$Ba_6F_4(Al_4F_{20})$ (117)	
	$Na_2Ba_3Cr_4F_{20}$ (88)	$AMnF_5 \cdot H_2O$ (107)				

Layer Structures

single layer				double layer		
type	bronze related	trans-terminal F	cis-terminal F	type	example	triple layer
A^IMF_4	β-$RbAlF_4$ "TTB" (118)	$TlAlF_4$ (89, 116, 128)	$NaCrF_4$ (120, 121)	$A^I_3M^{II}_2F_7$	$K_3Zn_2F_7$ (147)	$Cs_4CoCr_4F_{18}$ (153)
	$Cs_2NaAl_3F_{12}$ "HTB" (119)	NH_4FeF_4 (129–132)				
		$NaTiF_4$ (133)				
		$KFeF_4$ (134–137)				
		$RbFeF_4$ (138–140)				
		$CsFeF_4$ (141–143)				
		$AMnF_4$ (144, 145)				
$A^{II}MF_4$			$BaZnF_4$ (122–125)			
$A^I_2MF_4$		K_2NiF_4 (146–148)				
		$(BaF)_2ZnF_4$ (18, 149)				
$A^IA^{II}_2M_2F_9$			$CsBa_2Ni_2F_9$ (126, 127)			
$A^I_5M_3F_{14}$		$Na_5Al_3F_{14}$ (150, 152)				
		chiolites				

Framework Structures

type	example
AMF_3: perovskites	$NaNiF_3$, $NaCuF_3$ (154–156), $K_4Mn_3F_{12}$ (164)
	KMF_3, $KCuF_3$ (157–163), $Cs_2Ba_2Cu_3F_{12}$ (127, 164)
A_xMF_3: bronzes	$K_{0.6}FeF_3$ TTB (165, 166)
	$Cs_{0.2}Zn_{0.2}Fe_{0.8}F_3$ HTB (167, 168)
	$FeF_3 \cdot 0.33H_2O$ HTB (169)
$A^IM^{II}M^{III}F_6$: pyrochlores	$RbNiCrF_6$ (67, 170, 171)
	$CsAgFeF_6$, $NH_4Fe_2F_6$ (172–174)
	$CsNi_2F_6$ (175)
$A^I_2M^{II}M^{III}F_7$: weberites	Na_2MgAlF_7 (176–178), Na_2CuCrF_7 (127, 179)
	Na_2MnFeF_7 (180), Na_2CuFeF_7 (127, 179)
	$Fe_2F_5 \cdot 2H_2O$ (181–183)

[a] References are given in parentheses.

only attempts to summarize and update what has in this regard been amplified on fluorides in previous reviews.[5,10]

In fluorides of F:M < 6 stoichiometry it is rarely the CN which changes. What must therefore change is the connectivity of the octahedra, which now share their ligands instead of being isolated. There are many possible ways in which octahedra may be linked and the central cations bridged so as to produce polynuclear units. Such units are either of limited size and form separate oligomer groups or (which is more frequent among polynary fluorides) infinitely extended in one, two, or three dimensions. The bridges between the metallic centers may be single, double, or triple, corresponding to corner-, edge-, or face-sharing of octahedra.

The most important fluoride structure types with only corner-sharing are listed in Table IV. Most chain, layer, and framework structures belong to this group.

The group of structures containing doubly or triply bridged octahedra is considerably smaller, in spite of the fact that most of them in addition to edge- or face-sharing show corner-sharing of octahedra. Table VI gives some information on this group of compounds to be discussed later.

1. *Isotropically Linked [MF_6] Groups*

Only three-dimensional corner-sharing between identical [MF_6] groups, resulting in composition F:M = 3, leads to chemical and geometrical isotropy. Apart from the trifluoride structures,[9] this is found in the cubic AMF_3 compounds of the perovskite type and of the modified pyrochlore type, $RbNiCrF_6$.[170] Related to both but no longer strictly isotropic are the tetragonal (TTB) and hexagonal (HTB) tungsten bronze structures.[184,185] These are found for many fluorides $A_xM^{II}_xM^{III}_{2-x}F_6$,[10,165–169] but will not be treated here in detail, except for saying that mixed valency of the same element is not at all a prerequisite to form the structure.

a. Perovskites. Oxides of perovskite structure have often been the subject of systematic geometric considerations.[62,186,187] Table V shows that a radius/lattice constant relation analogous to that for the A_2BMF_6 elpasolites also applies to the AMF_3 perovskites, the corresponding parent structures. However, there are fewer fluoride representatives of cubic symmetry. Some noncubic perovskites falling outside the $0.88 \leq t \leq 1.00$ limits are also noted in Table V.

The reason for distortion outside this tolerance factor range is the lack of size fit. The type of distortion

TABLE V. Observed (a_o) and Calculated (a_c) Lattice Constants (pm) of Cubic Perovskites AMF_3[a]

		M[a]																			
		Mg		Ni		Zn		Co		Fe		V		Mn		Cd		Ca	
A[a]	r_c ($r_{Shannon}$)	67.5 (72.0)		69.0 (69.0)		71.7 (74.0)		72.8 (74.5)		76.1 (78.0)		76.6 (79)		80.7 (83.0)		91.0 (95)		95.2 (100)	
Cs	188.1 (188)	6L (HP)	1.074	2L	1.066	6L (HP)	1.051	9L	1.045	6L	1.029		1.026	6L	1.006	446.5	0.959	452.4	0.941
								413.8	1.000	418.8	0.984		0.982	425.1	0.962	446.4	1.000	452.5	1.000
Tl	174.4 (170)		1.027	6L	1.019	6L	1.006	413.5	1.001	418.3	1.001			425.0	1.000	439.5	0.917		0.900
																439.9	0.999		
NH_4	173.1 (–)		1.023	pseudocubic	1.015	411.6[i]	1.001[iii]	413.2	0.996	417.7	0.980		0.977	424.2	0.958	tetrag.	0.913		0.896
						411.3[ii]	1.001[iv]	412.9	1.001	417.7	1.000			424.4	1.000				
Rb	172.9 (172)	6L	1.022	6L	1.014	411.0 (LT)	1.001	412.7	0.995	417.2	0.979	418.2	0.977	424.2	0.958	439.9	0.913	445.5	0.896
						411.2	1.000	412.8	1.000	417.6	0.999	418.3	1.000	424.3	1.000	439.2	1.002	445.3	1.000
K	161.0 (164)	398.9	0.982	401.5	0.974	405.5	0.961	407.1	0.956	412.1	0.940	413.1	0.938	418.9	0.920	OR	0.877	OR	0.860
		399.5	0.998	401.7	1.000	405.6	1.000	407.2	1.000	412.0	1.000	412.7	1.001	418.7	1.000				
Ag	143.4 (–)	391.8	0.922	393.6	0.915	397.2	0.903	398.3	0.898		0.883		0.881		0.864		0.823		0.808
		391.2	1.002	393.4	1.001	397.3	1.000	398.9	0.998										

[a] For each M–A combination the data are tabulated as follows: (i) a_o, (ii) a_c, (iii) t, (iv) a_o/a_c. $a_c = 0.472r_A + 1.452r_M + 1.755r_F$, with r_F = 128.5 pm and adapted radii r_c as listed for the A^I and M^{II} cations. The corrected tolerance factors given, $t = 0.94t_c$, are based on $t_c = (r_A + r_F)/2^{1/2}(r_M + r_F)$ calculated with the same radii. The hexagonal perovskites occurring at $t > 1$ (upper left) are marked by the number of close-packed layers (L) within their identity period; the orthorhombic ones are designated by OR ($t < 0.88$, lower right). HP = high pressure phase, LT = low temperature phase. For observed lattice constants, see ref 6 and 10.

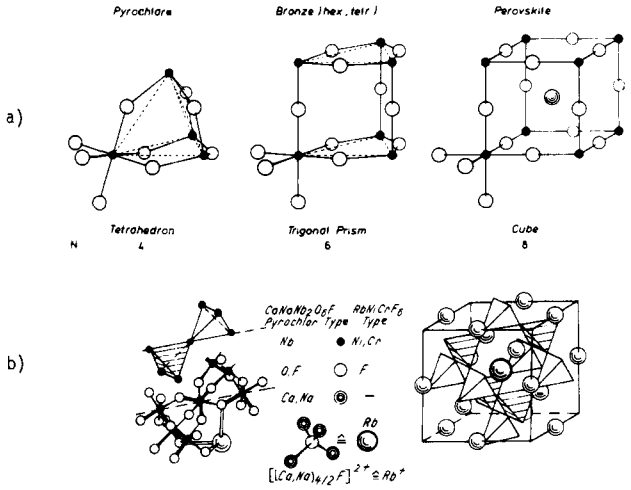

Figure 2. (a) Smallest units of N = 4, 6, and 8 octahedra in three-dimensional corner-sharing of the pyrochlore, bronze, and perovskite structures. (b) Arrangement of tetrahedral M_4 units in pyrochlores of $CaNaNb_2O_6F$ and $RbNiCrF_6$ types.

depends on the relative A cation size. If the cation is too small, $t < 0.88$, tilting of the octahedra occurs in order to restore at least some of the A–F contacts. The structures of the orthorhombic perovskites $NaMF_3$[154] and the monoclinic cryolites Na_3MF_6[40-42] are examples of this. The extreme case of $r_A \approx r_M$ ($t \approx 1/2^{1/2} = 0.71$), resulting in an ilmenite, i.e., an ordered corundum structure, has been found only in $LiZnF_3$.[188]

If the A cation is too large to fit in the cubic cell cage ($t > 1.0$), the M–F bonds become stretched, as is in fact observed in the high-pressure phases already mentioned.[78] However, when the compounds are prepared at normal pressure, energetically unfavorable M–F bond elongation is avoided by a martensitic transformation to hexagonal perovskite and elpasolite structures. In these, partial face-sharing of the octahedra occurs as a result of the stacking variation of close-packed AF_3 layers. While electrostatically these arrangements are not very favorable either, far more space is provided for the A cations between the strings of octahedra formed this way. This has been discussed elsewhere.[5,10,77,197]

In the cubic perovskite structure the $[MF_6]$ octahedra are directly linked via corners in all three dimensions (Figures 1 and 2). By contrast, in the elpasolites they are isolated by $[BF_6]$ octahedra, which link, however, the "complex" groups into the same kind of framework. Thus geometrically there is no essential difference between the two structures, except for the bond lengths, B–F and M–F, which contain all the important bond information. The ionic rigid-sphere approach used above is therefore sufficient to account for the cell dimensions of both the elpasolites and the perovskites. There is no need for further differentiation according to bond type, even in these extremes of isolated "complex" and three-dimensionally networked "coordination" compounds.

b. Pyrochlores. Isotropic three-dimensional corner-sharing of octahedra is also found in the M_2X_6 framework of the pyrochlores. The modified pyrochlore structure of the heterobimetallic fluoride $RbNiCrF_6$[170] differs from the structure of normal pyrochlores, like that of the mineral $CaNaNb_2O_6F$,[189] only by the number and size of the counterions. Thus Rb^+ in the first structure replaces $CaNaF^{2+}$ in the second. The sublattice of either kind is only incorporated to fill the

cavities inside the analogous M_2X_6 frameworks of both compounds, to which it is not specially bonded (see Figure 2). Quite recently, even a pyrochlore without any space fillers has been reported, viz., a new modification of FeF_3.[171]

Unlike in the perovskite framework, which contains one cavity (of CN 12) per MX_3 unit, in the modified pyrochlores two MX_3 units = M_2X_6 provide only one, still larger (CN 18) cavity. Consistent with these geometric conditions the modified pyrochlore structure is preferably adopted by cesium fluoro compounds $CsM^{II}M^{III}F_6$.[67] In the perovskites the smallest unit of three-dimensional linking consists of eight octahedra, centered at the corners of a cube (=the crystallographic cell). The cube contains the countercation A. In the pyrochlores the smallest unit comprises only four corner-sharing octahedra. The octahedral centers form a tetrahedron which remains empty, but four of these units are arranged once more tetrahedrally within the crystallographic cell and surround the countercations A as shown in Figure 2.

The tetragonal and hexagonal bronze structures already mentioned[184,185] are intermediate between the cubic and the tetrahedral array of octahedral centers, which here form trigonal prisms as the smallest units of three-dimensional linking. In between these units there are cavities of CNs 12 and 15 (TTB) and of 18 (HTB) for large A ions. However, the number of cavities is now reduced to 0.6 and 0.33 per MF_3 unit, respectively, and often even fewer are occupied.[167,190–192]

An interesting feature of the bronzes and of the cubic pyrochlores $AM^{II}M^{III}F_6$ is the random distribution of the di- and tervalent M cations over one and the same crystallographic equipoint. Only a limited number of noncubic pyrochlores are known, in which the different M cations are ordered. Surprisingly, all mixed-valence fluorides, like $NH_4Fe_2F_6$ or $CsNi_2F_6$,[172–175] belong to these ordered pyrochlores, of which at least two types exist.

Using a sample prepared from the iron fluorides with natural ^{57}Fe abundance and another enriched with $^{57}FeF_3$, a recent Mössbauer study has shown that the ion ordering in the orthorhombic mixed-valence $CsFe_2F_6$ proceeds via electron transfer.[193] The cubic, ionically disordered high-temperature phase can thus transform without cationic displacement at lower temperature to a phase of lower symmetry but with the M^{II} and M^{III} cations ordered. When M^{II} and M^{III} are different elements, this ordering mechanism by electron transfer cannot of course operate and the cubic pyrochlore structure is generally preserved. In this sense the cubic compounds are frozen high-temperature modifications. This is in accordance with their high molar volume, which is often higher than the molar volume sum of the binary components.

The existence of a clear-cut radius/lattice constant relation for the cubic pyrochlores $CsM^{II}M^{III}F_6$ has already been mentioned.[67] It should be noted that isostructural oxides $CsM^{V}M^{VI}O_6$ and all intermediate compositions of oxide fluorides CsM_2X_6 (X = O, F) are also known.[194]

2. Anisotropically Linked [MF_6] Groups

When not all the corners of octahedra are linked in the same way or when edges or faces are shared between the octahedra, the bonding, structure, and physical properties become more or less anisotropic. This is often indicated by the formation of chain and layer structures, which according to Tables IV and VI vary widely depending on geometry-related factors like composition and relative ionic sizes. In addition, anisotropy may be introduced through electronic and electrostatic effects. Examples are the d^4 and d^9 configurations or other Jahn–Teller systems, or heterobimetallic compounds containing transition-metal ions of different charges. Some relevant principles will be shown in the following.

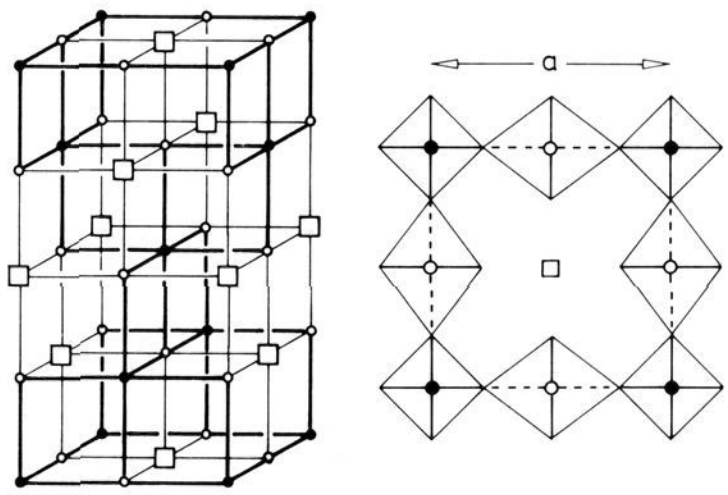

Figure 3. Order of octahedral vacancies in the framework structure of the cation-deficient perovskites $K_4Mn_3F_{12}$[164] and $Cs_2Ba_2Cu_3F_{12}$[179] and the chiolite-like arrangement of Jahn–Teller-elongated octahedra in its basal plane.

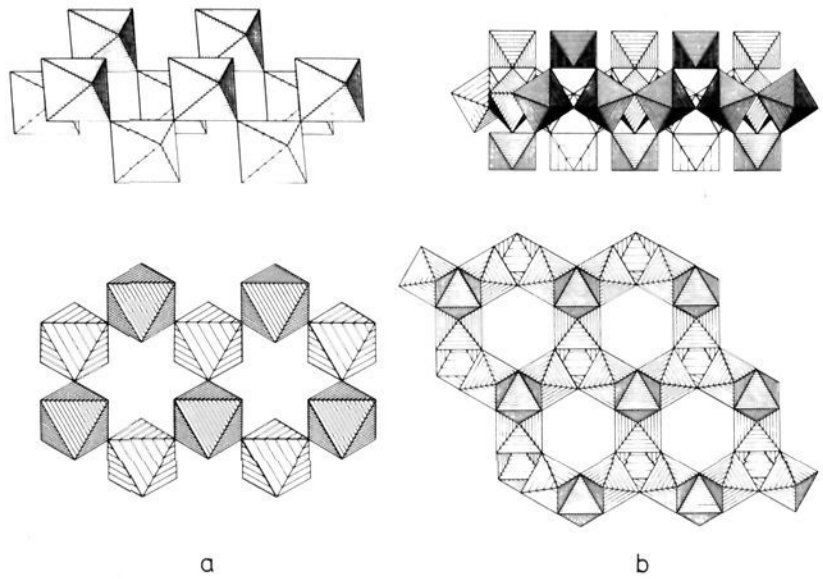

Figure 4. (a) Puckered layer structure of $CsBa_2Ni_2F_9$,[126] a cation-deficient hexagonal perovskite (rhombohedral 9L structure). (b) Triple-layer structure of $Cs_4CoCr_4F_{18}$, deriving from the pyrochlore framework. In both layer types, a and b, each shown in different projections, the octahedra have three fac-terminal ligands at the sheets' surfaces.

a. Single Bridges: Corner-Sharing Only. In the compositional F:M range between 3 and 4 the double- and triple-layer structures of $K_3Zn_2F_7$[147] and $Cs_4CoCr_4F_{18}$[153] are found, deriving from the perovskite and pyrochlore structure, respectively (cf. Figure 4b). The largest group in this range, however, is that of the weberites $A_2M^{II}M^{III}F_7$ (A = Na, Ag),[10,195] which form framework structures. At least two structural variants exist,[176–180] but in all of them it is the higher charged cation M^{III} which retains two of its ligands unshared (cf. Figure 14). The difference involves the position, cis or trans, of these terminal ligands. It depends on the chain directions of the M^{II} ions, which form 60° rotated or parallel rows of trans corner-sharing octahedra, interconnected by the M^{III} ions.

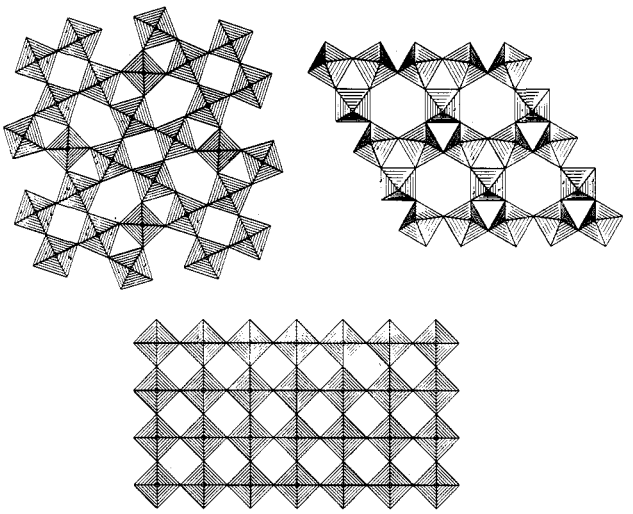

Figure 5. Projection of the layers present in the tetragonal and hexagonal bronze-related layer structures of β-$RbAlF_4$[118] and $Cs_2NaAl_3F_{12}$,[119] compared to the more usual square mesh layer.

Essentially the same octahedral network as in the orthorhombic weberites is found in $Fe_2F_5 \cdot 2H_2O$[181,182] and other $M^{II}M^{III}F_5 \cdot 2H_2O$ hydrates.[183,196] However, since the trans-terminal aquo ligands are located here at the lower charged M^{II} cations, these hydrates were called inverse weberites.

The compositional range $4 \leq F:M \leq 5$, richer in fluorine, permits a framework structure which is shown in Figure 3 and which is encountered only in the exceptional cases of the Jahn–Teller-stabilized cation-deficient perovskites $Cs_2Ba_2Cu_3F_{12}$ and $K_4Mn_3F_{12}$.[164] Normally layer structures are formed, of which the chiolites $Na_5M_3F_{14}$[150-152] and compounds like $CsBa_2Ni_2F_9$[126,127] are the fluorine-richest examples (Figure 4a). The latter are cation-deficient hexagonal perovskites deriving from the 9L-$CsCoF_3$ structure.[193,197]

The typical F:M proportion for most layer structures is 4, realized in many variants. Some main distinctions concern the positions of the two terminal ligands, cis or trans, the relative orientation of different layers, and the form of meshes within the layers. Triangles, pentagons, and hexagons are found in the bronze-related layer types[118,119] shown in Figure 5, but only square meshes are present in the majority of cases[128-149] (see Table IV). Nevertheless, there remain many differences, which depend on the relative tilting of the octahedra within the layers. The same problem, giving rise to a variety of phase transitions,[136,139,140,143] is known from the perovskite family of structures, where it has been systematically treated by Glazer.[198,199] This treatment of tilting modes was applied to layer structures quite recently.[200]

If short sections of AMF_4 layer structures are curled up, which is made possible by the all-cis connection of three parallel strands, even a chain structure may be achieved for this composition, F:M = 4. Such a triple-chain structure (Figure 6) has been observed in a tilted and an untilted version in the chromium compounds $KCrF_4$[112,113] and $CsCrF_4$[114-116], respectively.

One of the strands of the triple chain separated is the usually found single chain of composition F:M = 5 (cf. Figure 7). Several variants of such trans-connected chains of octahedra are known.[89-107] An important distinction may be made according to the packing of

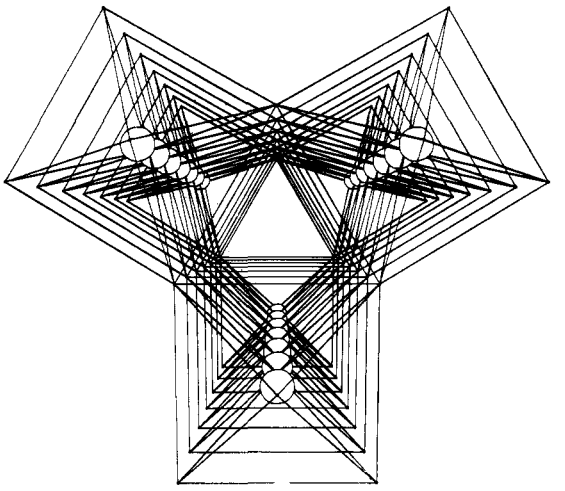

Figure 6. Triple-chain structure of $CsCrF_4$,[114] seen along the threefold channel.

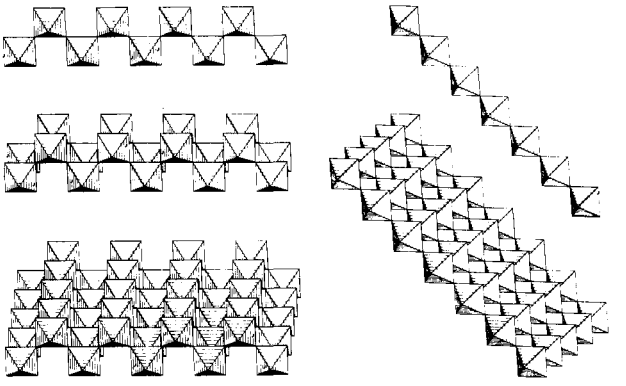

Figure 7. Idealized cis- and trans-connected chains, double chains, and layers of octahedra in polynary fluorides of composition A_mMF_5, $A_mM_2F_9$, and A_mMF_4, respectively.

chains, which in manganese(III) compounds was found to be either tetragonal or (pseudo)hexagonal.[95]

Another kind of chain structure is realized by continued cis bridging, resulting in zigzag chains of a sometimes helical array, as found in the $SrFeF_5$ structure.[83] Alternative cis and trans bridging has been observed in the hydrate $Ba_4Fe_3F_{17} \cdot 3H_2O$, containing, besides FeF_5^{2-} chains, isolated FeF_6^{3-} octahedra.[201] The unique $BaFeF_5$ structure is composed of a simple and a "winged" trans chain.[103,106]

Joining two parallel cis-bridged chains leads to double-chain structures of composition F:M = 4.5, intermediate between say the chain structure of $BaGaF_5$[84] and the layer structure of $BaZnF_4$,[122] as shown schematically in Figure 7 on the left. Several structural variants are known, containing either differently charged M ions, e.g., in Ba_2ZnAlF_9, or A ions, e.g., in $KPbCr_2F_9$.[108-111] But the resulting double chain, which forms a zigzag band, is essentially the same in all these cases, except for a unique meander string in the $[O_2]$-Mn_2F_9 structure.[202] It should be remembered, however, that a $[M_2F_9]$ composition leading to a layer structure has already been mentioned in the example of $CsBa_2Ni_2F_9$.[126] The other extreme, an isolated pair in $Cs_3Fe_2F_9$,[203] will be noted in the following section. A common feature of all these $[M_2F_9]$ compounds and of the $Cs_4CoCr_4F_{18}$ structure as well[153] is the occurrence of octahedra with three terminal ligands in facial position (cf. Figures 4 and 8). The corresponding M–F bonds

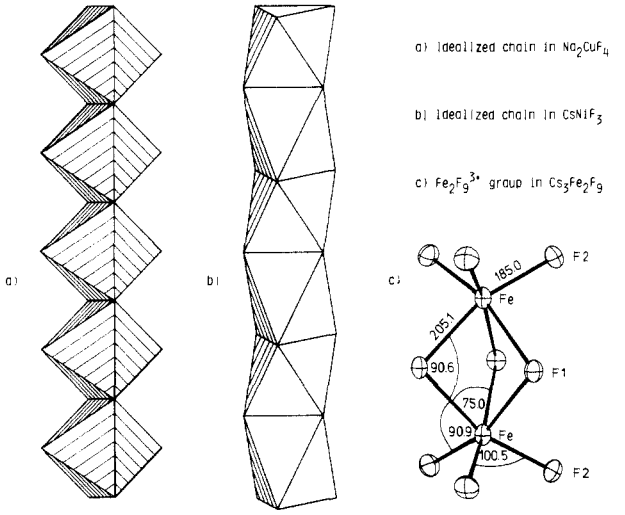

Figure 8. Chains of edge- and face-sharing octahedra, as found in the structure types of Na_2CuF_4[204] and $CsNiF_3$,[197] respectively. Extreme cation–cation repulsion (Fe–Fe = 291.6 pm) is observed in the binuclear chain fragment of $Cs_3Fe_2F_9$.[203]

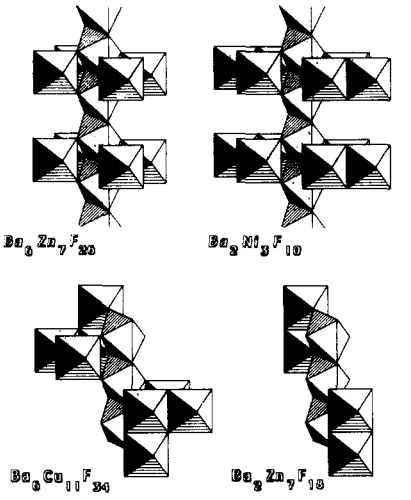

Figure 9. Edge-sharing octahedral units in some phases of BaF_2–MF_2 systems (reproduced from ref 221, with permission).

are considerably shortened.

b. Multiple Bridges. The pure forms of either edge- or face-sharing of octahedra are known only from the structure types of Na_2CuF_4[204] and $CsNiF_3$,[193,197] respectively. Both are chain structures. The first (F:M = 4) contains two trans-terminal ligands, perpendicular to the chain direction of trans edge-sharing octahedra. In the other chain structure (F:M = 3), formed by octahedra sharing opposite faces, all ligands are bridging. The binuclear structure of $Cs_3Fe_2F_9$[203] just mentioned is a segment of the $CsNiF_3$ structure, i.e., its cation-deficient variant, also illustrated in Figure 8.

More recently, a variety of layer and framework structures have been found, most of them lying in the compositional range $3 \leq F:M \leq 4$, in which corner-sharing occurs in addition to edge- or face-sharing. These fluorides are listed in Table VI. It is noticeable that face-sharing is observed exclusively in the cesium compounds, whereas most of the edge-sharing structures happen to be barium compounds.

i. Edge-Sharing. Edge-sharing in combination with corner-sharing is well-known from the rutile structure of the difluorides. In the rutiles parallel chains of trans-edge-connected octahedra as in Na_2CuF_4 are highly condensed to make each ligand 3-coordinated. This is a high CN for a fluoride ion with respect to a transition metal. It is also observed for some of the anions in the structures forming in the BaF_2–MF_2 systems.[208,212,213,220,221] As listed by Ferey, the number of 3-coordinated ligands increases from 8% in $Ba_6Zn_7F_{26}$ (F:M = 3.71)[208] to 33% in $Ba_2Zn_7F_{18}$ (F:M = 2.57),[221] parallel to the decrease in F:M proportion (Table VI). It is interesting to note that terminal ligands (CN 1) also occur in all these compounds except in the last-mentioned one. However, the majority of anions are 2-coordinated, as is usual in this compositional range.

Only Cr_2F_5 and $MnAlF_5$[222,223] and some of the ternary BaF_2–MF_2 fluorides contain the infinite and linear chains of trans edge-sharing octahedra of the parent rutile structure. For example, in α-$Ba_2Cu_5F_{14}$[220] the infinite chain is zigzag by consecutive cis-trans-sharing of edges as known for instance from the $ZrCl_4$ structure.[230] In addition, or alternatively, bi-, tri-, and tetranuclear edge-sharing units are found in other of these

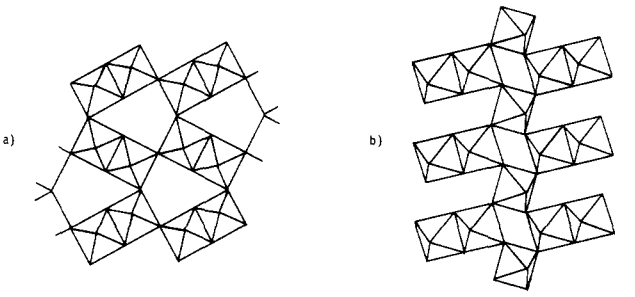

Figure 10. Binuclear edge-sharing groups in (a) the framework structure of NH_4MnFeF_6[217] and (b) the layer structure of $Ba_2CuV_2F_{12}$.[205]

interesting barium compounds; some of them are shown in Figure 9. Their structures are related by crystallographic shear and ordered defects to the rutile and rock salt types, as discussed and well-illustrated by Ferey.[221]

Compared to the rather complex structures in the BaF_2–MF_2 systems, the heterobimetallic transition-metal compounds in this series of edge-sharing structures are of simpler construction. At F:M = 3 there is, for example, $NaMnCrF_6$,[215] which has an ordered Na_2SiF_6 type structure,[29,30] like many similar compounds.[10,214,216] NH_4MnFeF_6[217–219] is structurally related to HT-$BaTa_2O_6$.[231] In its structure edge-sharing binuclear $[MnFeF_{10}]$ groups rather than single octahedra are connected via the remaining corners to form a three-dimensional framework. The same principle of course permits the construction of a layer structure. It has been found recently in a modified form in $Ba_2CuV_2F_{12}$ (F:M = 4): binuclear units $[CuVF_{10}]$ (Figure 10) are two-dimensionally interconnected by single $[VF_6]$ octahedra, with all the axes perpendicular to the resulting layer bearing terminal ligands.[205]

The intermediate composition F:M = 3.5 in the compounds $BaM^{II}Fe^{III}F_7$ leads to related framework structures for M^{II} = Mn, Cu, and Zn, all of which contain binuclear $[M_2F_{10}]$ units.[209–211] In the copper and zinc compounds these are the only units (each with two terminal ligands trans to the plane of the cations and the common edge). Partial cation disorder is observed in the copper compound.[210] The manganese compound, $BaMnFeF_7$,[209] however, is a combination of $[Mn_2F_{10}]$ double and $[FeF_6]$ single octahedra. The terminal ligands here are located cis to the higher valent Fe^{III} ion

TABLE VI. Fluoride Crystal Structures Containing Groups of *n* Octahedra Joined by Multiple Bridges

double bridges (edge sharing)				triple bridges (face sharing)			
F:M	*n*		ref	F:M	*n*		ref
			Isolated Pair				
				4.5	2	$Cs_3Fe_2F_9$	203
			Chain Structures				
4	∞	Na_2CuF_4	204	3	∞	$CsNiF_3$(2L)	193, 197
			With Additional Single Bridges (Corner Sharing)				
			Layer Structures				
4	2	$Ba_2CuV_2F_{12}$	205	3.75	2	$Cs_7Ni_4F_{15}$	224
3.5	3	$BaMnGaF_7$[a]	206, 207	3.33	3	$Cs_4Ni_3F_{10}$	193, 225
				3.2	5	$Cs_6Ni_5F_{16}$	226
			Framework Structures				
3.71	∞	$Ba_6Zn_7F_{26}$	208				
3.5	2	$BaMnFeF_7$	209				
		$BaCuFeF_7$	210				
		$BaZnFeF_7$	211				
3.33	∞	$Ba_2Ni_3F_{10}$	212	3	2	$CsMnF_3$(6L)	193, 227
3.09	3	$Ba_6Cu_{11}F_{34}$	213		3	$CsCoF_3$(9L)	193, 197
3	∞	$NaMnCrF_6$	214–216		3	Cs_2MnNiF_6(12L)	228
3	2	NH_4MnFeF_6	217–219		4	$Cs_5CdNi_4F_{15}$(10L)	229
2.8	2+∞	α-$Ba_2Cu_5F_{14}$	220				
2.57	3+4	$Ba_2Zn_7F_{18}$	221				
2.5	∞	Cr_2F_5, $MnAlF_5$	222, 223				

[a] Edge sharing between $[GaF_6]$ and $[MnF_6]$ polyhedra.

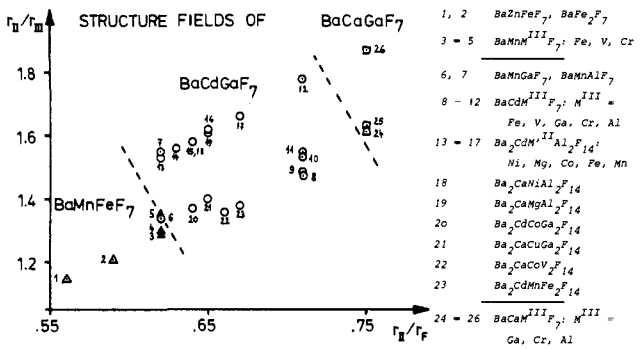

Figure 11. Radius ratio dependent structure fields of $BaMnFeF_7$,[209] $BaCdGaF_7$[206]/usovite[207] and $BaCaGaF_7$[59] type fluorides.

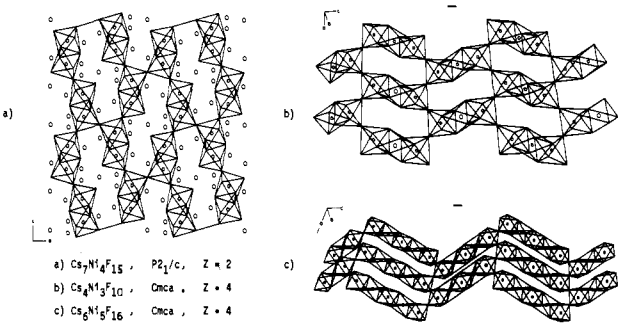

Figure 12. Bi-, tri-, and pentanuclear groups of face-sharing octahedra in some layer structures of $CsF–NiF_2$ phases.[193,224,226]

only, similar to the situation in the trigonal weberite Na_2MnFeF_7.[180]

A special feature of the $BaMnGaF_7$ layer structure,[206] also noted in Table VI, is the higher CN 8 of half the manganese cations. By size-differentiating substitution of these cations many isostructural fluorides have been obtained.[207,232] They later were named "usovites", according to the mineral $Ba_2CaMgAl_2F_{14}$,[233] previously synthesized by Nature.

Another structural type, $BaM^{II}M^{III}F_7$ with M^{II} exclusively 8-coordinated, is formed by calcium compounds $BaCaM^{III}F_7$.[59] The occurrence of the three main types mentioned here depends on both the $r(M^{II})/r(M^{III})$ and $r(M^{II})/r(F)$ radius ratios, as illustrated in Figure 11.

ii. Face-Sharing. The cesium compounds with F:M = 3 listed in Table VI are all "hexagonal perovskites", viz., the stacking variants between the cubic form (close-packed layer sequence ABC = 3L) and the simple hexagonal packing as shown by the $CsNiF_3$ chain structure (sequence AB = 2L)[197] (cf. Figure 8). The geometric reason for this structural variety has already been discussed in terms of the tolerance factor. The resulting structures, which exhibit enlarged identity periods (6L, 9L, 10L, 12L), are characterized by polynuclear groups of 2, 3, and 4 face-sharing octahedra, interconnected by corner-sharing, sometimes via single octahedra.[10]

In addition to the one-dimensionally widened framework structures formed in this way by AMF_3 compounds, three related layer structure types have been found in the compounds $Cs_7Ni_4F_{15}$, $Cs_4Ni_3F_{10}$, and $Cs_6Ni_5F_{16}$.[224–226] They contain the chain fragments of 2, 3, and 5 face-sharing octahedra shown in Figure 12 (see Table VI). These units are only two-dimensionally linked by corners and at the same time, according to the composition F:M > 3, some ligands are terminal.

Because of M–M cation repulsion, edge- and still more face-sharing is unfavorable from an electrostatic point of view.[1,2] As a consequence the octahedra become strongly distorted and the M cations are off center, unless subject to symmetrical forces inside longer chains.

For face-sharing octahedral units in CsF/MF_2 systems the structural results for 14 compounds, belonging to 6 structure types, are compiled in Table VII.[193,234] The varying M–M and M–F distances yield comparable figures R, if octahedral distortion and cation–cation repulsion are expressed by the ratio R = M–M/M–F, also listed in the table. The ideal value is $R = 2/3^{1/2} = 1.155$ for undistorted octahedra.

TABLE VII. Ternary Fluorides Forming in CsF/MF_2 Systems: M-F and M-M Distances (pm) and Ratio R = M-M/M-F within units of N Face-Sharing Octahedra Found for the Compounds[193,234]

N = 2				N = 3				N =5				N = ∞			
	R	M-F	M-M		R	M-F	M-M		R	M-F	M-M		R	M-F	M-M
$RbMgF_3$	1.38	201.0	278.2	HP-$CsNiF_3$[a]	1.33	203.4	270.7					NP-$CsNiF_3$[b]	1.30	201.3	262.1
$ACoF_6$[c]	1.37	206.1	281.7	$CsCoF_3$	1.34	206.1	275.3								
$CsFeF_3$	1.39	210.2	292.3												
$CsMnF_3$	1.40	214.0	299.5	$Cs_4Mg_3F_{10}$	1.37	200.9	274.8								
$Cs_7Ni_4F_{15}$	1.37	203.7	278.2	$Cs_4Ni_3F_{10}$	1.34	202.8	272.7	$Cs_6Ni_5F_{16}$	1.32	201.9	267.2				
				$Cs_4Zn_3F_{10}$	1.36	205.1	279.4								
$Cs_7Co_4F_{15}$	1.37	206.5	283.5	$Cs_4Co_3F_{10}$	1.35	205.7	277.9								

[a] High-pressure phase (9L). [b] Normal-pressure phase (2L). [c] A = $Cs_{0.37}Rb_{0.63}$ (6L phase).

The results in Table VII show that—independent of cation and structure type—the M–M repulsion is most pronounced in dinuclear units of face-sharing octahedra (N = 2: $1.40 \geq R \geq 1.37$) and least in an infinite chain ($N = \infty$: $R = 1.30$). The tri- and pentanuclear cases are intermediate (N = 3: $1.37 \geq R \geq 1.33$; N = 5: $R = 1.32$). It is interesting to note that the closed-shell ions Mg^{2+} and Zn^{2+}, which are incapable of d–d interactions, define the upper limit in $Cs_4M_3F_{10}$ compounds. However, the overall gradation observed is as would be expected from simple electrostatic principles, which also account for the unusually shortened F–F and elongated M–F distances with respect to the shared faces.

The coexistence of face- and corner-sharing in most of these structures is important for the magnetic properties of the corresponding transition-metal compounds and the intercationic distances are of interest in the same context of magnetic interactions.[4]

IV. Bond Valences in Octahedrally Coordinated Fluoro Compounds

A. Length and Strength of Bridging and Terminal M–F Bonds

Interatomic distances, nowadays accessible by diffraction methods with high precision, reflect the equilibrium situation between bonding interactions and repulsive forces of all particles within a crystal. Though remarkable progress has been made in quantum mechanical ab initio calculations, prediction of detailed structural properties like bond lengths and bond strengths in complex inorganic solids is not yet within reach. Deductive methods based on experimental structure data remain therefore more helpful. One such attempt is the calculation of the Madelung parts of lattice energy (MAPLE), successfully applied to numerous structures mainly by Hoppe.[235] Another approach, which will be treated here more thoroughly, is the calculation of "empirical" bond strengths, usually called bond valences, from experimental bond lengths. For chemists it is, on the one hand, in many cases more informative to know the strength of a bond rather than its length. On the other hand, bond strengths or bond lengths of unknown compounds may be derived, once an adequate parameter set has been fixed.

The method of calculating bond valences introduces a "normalization" effect which permits one to compare, for example, the same complex anion in different structural environments or different complex anions in related structures. This method thus offers the possibility of separating different structural effects, like that of bridging and that of electronic configuration.

TABLE VIII. L(max) (pm) and $2k$ Parameters for Bond Strength Calculations with Fluorides

ion	L(max)	$2k$	ion	L(max)	$2k$
Li^+	257	1.11	Al^{3+}	218	0.82
Na^+	309	1.43	Ga^{3+}	226	0.81
K^+	325	1.17	In^{3+}	287	1.80
Rb^+	341	1.17	Tl^{3+}	262	1.02
Cs^+	350	0.92			
Tl^+	325	0.60	Sc^{3+}	260	1.3
			V^{3+}	240	1.08
Be^{2+}	208	1.11	Cr^{3+}	228	0.86
Mg^{2+}	252	1.17	Mn^{3+}	232	0.89
Ca^{2+}	299	1.34	Fe^{3+}	232	0.89
Sr^{2+}	310	1.15			
Ba^{2+}	334	1.01	Ti^{4+}	239	1.14
			V^{4+}	238	1.17
Cr^{2+}	256	1.08	Mn^{4+}	216	0.78
Mn^{2+}	259	1.08			
Fe^{2+}	253	1.06	V^{5+}	226	0.99
Co^{2+}	254	1.16			
Ni^{2+}	232	0.78			
Cu^{2+}	239	0.81			
Zn^{2+}	203	0.78	Cd^{2+}	301	1.43

For example, the magnitude of Jahn–Teller distortions may be ascertained from comparisons with the normalized bond valences of suitable model compounds which are not affected by electronic degeneracy, provided the crystal structures in both series have been determined accurately.

The empirical bond strength calculations, first performed by Pauling[236] in 1947 on the bond length–bond order relation of C–C bonds, have been extended, with modifications (mainly for oxide structures), since 1970 by Zachariasen,[237] Donnay and Allmann,[238,239] Brown, Shannon, and Altermatt,[240–242] Trömel,[243] and others. We apply the method of Donnay and Allmann to the treatment of fluoride structures. The method is based on a parameter set which we newly calculated for metal–fluorine bonds (Table VIII). In the following paragraphs we present a short survey of the method of determining M–F bond valences as well as some examples to illustrate the effect of structural dimensionality, countercations, and electron configuration, in particular of the Jahn–Teller effect.

B. Calculation of Bond Valences

The most common methods of calculating empirical bond strengths or "bond valences" from bond lengths use essentially the same logarithmic relation with two adjustable parameters:

$$v = 10^{((L(1)-L)/2k)} \quad \text{(1) Donnay and Allmann}^{239} \text{ (D\&A)}$$

$$s = \exp(r_0 - r)/B \quad \text{(2) Brown and Altermatt}^{242} \text{ (B\&A)}$$

TABLE IX. Bridging and Terminal Bond Lengths (pm) and Relative Bond Valences v_r Varying with Bridging Type

type of bridge	compd		mean bond length: bridge	mean bond length: terminal	mean v_r: bridge	mean v_r: terminal	ref
		I. Two Single Bridges (Chain Structures)					
trans	$Rb_2AlF_5 \cdot H_2O$		188.7	178.3	0.82	1.09	90
cis	Rb_2FeF_5		204.4	189.2	0.76	1.13	82, 244
	Rb_2CrF_5		199.0	186.7	0.79	1.13	81
		II. Four Single Bridges (Layer Structures)					
trans terminal	$CsFeF_4$		196.2	186.1	0.91	1.18	141
	$Cs_2NaAl_3F_{12}$		182.8	174.8	0.92	1.16	119
cis terminal	$NaCrF_4$	trans	192.7	186.1	0.95	1.13	120
		cis	193.6		0.93		
	$NaFeF_4$	trans	195.5	187.4	0.93	1.14	121
		cis	195.6		0.93		
		III. Triple Bridge (Dimeric M_2F_9 Anion)					
facial	$Cs_3Fe_2F_9$		205.1	185.0	0.75	1.25	203

where v or s is the bond valence, $L(1)$ or r_0 is the "reference bond length" parameter (Å), L or r is the experimental bond length (Å), and $2k$ or B is a parameter mainly responsible for the curvature of the bond length/bond valence curve, where $2k = B/\log(e)$.

The sum of bond valences around each atom in a structure should be close to its formal charge.[1] This follows from the electrostatic valence concept and may be used as an internal consistency test.

The main difference between the methods of D&A and B&A concerns the philosophy of choosing the two parameters. In his recent paper[242] Brown prefers the choice of "universal" parameters r_0 and B. B is kept at a constant value of 0.37, while r_0 is fitted by least-squares for each bond type (e.g., Al–O) from a large number of crystal structure data. The price to pay for introducing a *single* parameter for a whole class of compounds covering a wide range of compositions and crystal structures is the loss of individual precision. It therefore is not surprising that considerable deviations of bond-valence sums from the formal charge occur in some cases for both cations and anions.

Allmann derives the $2k$ parameter for individual bond types (e.g., Al–O). The second, more sensitive parameter $L(1)$ is fitted individually for each coordination polyhedron (Figure 13). This procedure leads to a normalization effect: the sum of bond valences from a cation to all coordinated anions becomes equal to the formal charge. The individual precision of the bond valences v so obtained is higher, but at the expense of universal significance and the number of parameters. In spite of this we think them more suitable than Brown's values for comparison of individual distortions when related complex anions like MF_6^{n-} are involved. A justification for individual fitting of the parameter $L(1)$ follows from the fact that the observed M–F distances in fluorides show good constancy and are not significantly affected by individual distortions of the octahedra.

For the most common metal–fluorine bonds we have calculated the parameters $2k$ according to Allmann,[239] using the ionic radii dependence on coordination number as documented in Shannon's[64] table. First, a "maximum ionic radius" $r(\max)$ was defined by a linear extrapolation to $v_0 = 0$ from a plot of ionic radius at different coordination numbers versus the ideal electrostatic valence $v_0 = q/CN$ (q = charge of cation). The sum of the cation $r(\max)$ values and that of the fluoride ion (1.35 Å) yields the maximum bond lengths $L(\max)$,

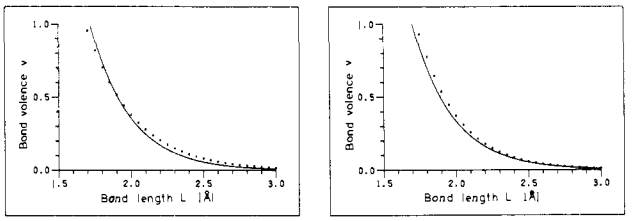

Figure 13. Influence of the parameters $2k$ and $L(1)$ on the bond length/bond valence curve. (a) Solid line, $2k = 0.63$; dotted line, $2k = 0.75$, $L(1)$ fitted for $\bar{L} = 1.89$ Å. (b) Solid line, $L(1) = 1.70$, $2k = 0.63$; dotted line, $L(1) = 1.73$ Å, $2k = 0.63$.

from which the $2k$ parameter may be calculated (Table VIII):

$$2k = \ln 10(L(\max) - L)$$

The mean bond length L is given by the sum of Shannon's ionic radii or, alternatively, by experimental mean values based on reliable crystallographic determinations of fluoride structures.

As might be expected, considerable deviations occur from the corresponding parameters in oxide structures. To test the internal consistency of the parameter set, sums of bond valences have been calculated, for a large number of polynary compounds, over all the bonds pointing at each F^- anion. For the fluoride ion a sum of 1 should result, corresponding to its formal charge. In all the cases we have included in the calculations, the individual deviation from the ideal value was smaller than 6%, except for A_2MF_4 compounds (up to 15%), where indeed the structural behavior shows anomalies (see section C).

Since the sum of bond valences v within a coordination polyhedron is normalized to the formal charge of the central cation, polyhedra with different charge may not be compared directly. This becomes possible, however, by using "relative bond valences" $v_r = v/v_0$ (v_0 = "ideal" bond valence in an undistorted polyhedron).

C. Effect of Structural Dimensionality

It is well-known that the bond length involving a bridging ligand is usually longer than one involving a terminal ligand. A look at the relative bond valences gives a more quantitative insight into the extent of bond weakening on formation of the different kinds of ligand bridges. Table IX lists selected examples for the principal bridging types discussed in the previous sections.

TABLE X. Effect of Countercations on the Relative Bond Valences of Bridging and Terminal Bonds

weak effect					stronger effect			
		mean v_r				mean v_r		
compd		bridge	terminal	ref	compd	bridge	terminal	ref
			Cis-Chain Structures					
Rb_2CrF_5		0.79	1.10	81	$BaCrF_5$	0.89	1.05	86
Rb_2FeF_5		0.76	1.12	244	$SrFeF_5$	0.90	1.05	83
K_2FeF_5		0.78	1.11	80				
			Trans-Chain Structures					
$Rb_2AlF_5 \cdot H_2O$		0.82	1.09	90	$CaCrF_5$	0.90	1.05	102
			Cis–Trans Layers					
$NaFeF_4$	trans	0.93	1.05	121	$BaCoF_4$	0.87	1.11	124
	cis	0.93				1.02		
			K_2NiF_4 Type Layers					
Rb_2MgF_4		0.98	1.05	245	K_2MgF_4	1.01	0.98	147
Rb_2CoF_4		0.97	1.06	245	K_2CoF_4	0.99	1.02	147
Rb_2NiF_4		0.96	1.07	245	K_2NiF_4	0.995	1.01	147

To exclude anisotropic effects of electronic configuration only compounds of main-group elements or transition-metal ions exhibiting "isotropic" occupation of d orbitals like Fe(III) or Cr(III) have been chosen. The effect of the countercations is kept at a minimum by selecting model compounds with large differences in charge and in ionic radius, i.e., preferably fluorometallates(III) of the largest alkali-metal ions.

It is obvious from the figures given in Table IX that the weakening of the bridging bonds is correlated with the dimensionality of the structure. In linear-chain structures built up from octahedra sharing corners, the bridge-weakening effect is about 20% and seems to be somewhat stronger for the cis than for the trans connection. Compared with the overall mean bond length the elongation reaches about 10 pm. In the typical $TlAlF_4$-related layer structure of $CsFeF_4$ the four bridging bonds are less elongated and weakened by only half this amount (about 9%). The still smaller effect in the sodium compounds containing layers of cis–trans connected octahedra may be due not only to the different bridging type but also to the effect of the smaller countercation. This will be discussed later on.

For double bridges no simple model compounds have been found. In fluorides, chains of octahedra sharing edges are known only with Jahn–Teller ions or as a part of structures with 3-dimensional networks like the rutiles (see Figures 8 and 9). The bond valence in such a bridge is expected to be somewhat more reduced than in a chain of octahedra sharing vertices.

The extreme bond valence reduction in the triple bridge of $Cs_3Fe_2F_9$ reflects the strong cation–cation repulsion within the binuclear complex anion.

D. Effect of Countercations

If we pass from the cesium and rubidium fluorometalates(III) to corresponding $A^I_xM^{III}F_{3+x}$ or $A^{II}_xM^{III}F_{3+2x}$ compounds containing smaller or more highly charged A cations of the alkali-metal and alkaline-earth groups, respectively, the effect of the A cations becomes the more important the more the A–F bonds approach the strength of the M–F bonds. Of course, the low dimensionality of the MF_{6-n} substructure, which is responsible for the optical, electric, and magnetic properties and therefore generally more interesting, remains unchanged. But the bonding network including the "inert" A cations becomes increasingly

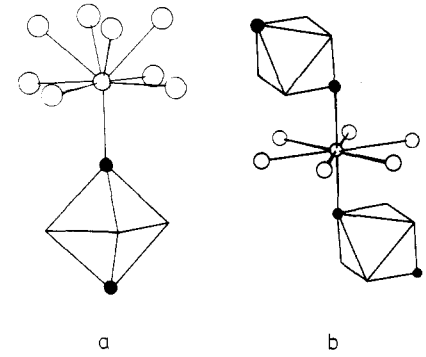

Figure 14. (a) 1+8 coordination around K in compounds K_2MF_4. (b) 2+6 coordination of Na in weberites $Na_2M^{II}M^{III}F_7$. In both cases the short A–F bonds point to terminal ligands (full circles) of MF_6 octahedra.

three-dimensional in character. As a consequence, the differences between bridging and terminal bonds in the MF_6 octahedra (cf. Table IX for examples nearly undisturbed by the A cations) now begin to disappear or, in special cases, even to reverse. If we look at the cis- or trans-connected chain structure compounds of Table X, the formal replacement of the two large alkali-metal cations by an alkaline-earth cation leads, in terms of bond valences, to only half the octahedral distortion.

"Cis–trans-connected" layered structures are known only for sodium or barium and, one case, for a strontium compound. Thus, as expected for these countercations, the octahedral distortion is small. Greater differences in the individual bond lengths and valences may be attributed to the irregular coordination around the cations mentioned. An extreme example of countercation effect is found in the layer structures of the K_2NiF_4 type. Although potassium is an alkali-metal cation medium or even large in size, the MF_6 octahedra in the K_2MF_4 compounds (M = Mg, Mn, Co, Ni, Zn)[147] are nearly regular, irrespective of the different nature of the bridging and terminal ligands. This strange behavior may be understood if we look at the "1+8" coordination of the potassium ions (Figure 14). One strong K–F bond—the bond valence of which is about half as high as for the M–F bonds—is directed in a linear grouping K–F–M toward a terminal fluoride ion. By symmetry, the same geometry obtains for the terminal ligand at the opposite side of the layer. This contrapolarization or even bridging by strong K–F bonds strongly weakens the "terminal" M–F bonds

TABLE XI. Octahedral Distortion in Terms of Bond Lengths (pm) and Relative Bond Valences v_r in Rutiles MF_2

metal	d electrons	ionic radius[64]	$d(M-F)_{ax}$	$d(M-F)_{eq}$	d_{ax}/d_{eq}	$v_{r(ax)}$	$v_{r(eq)}$	ref
Mg	d^0	72	198.0	199.7	0.991	1.022	0.989	251
V	d^3	79	207.3	209.2	0.989	1.027	0.986	252
Cr	d^4	80	243.0	199.5	1.218	0.495	1.252	253
Mn	d^5	83	210.4	213.1	0.987	1.039	0.981	253
Fe	d^6	78	199.8	211.8	0.943	1.181	0.910	253
Co	d^7	74.5	202.7	204.9	0.989	1.029	0.985	253
Ni	d^8	69	198.1	202.2	0.980	1.082	0.959	253
Cu	d^9	73	229.8	192.5	1.194	0.442	1.279	254
Zn	d^{10}	74	201.2	204.6	0.983	1.068	0.966	253

subject to a kind of mutual electrostatic "trans effect". In the isostructural rubidium compounds this influence is reduced by the increase in ionic size.

On the other hand, in sodium compounds a similar but still more pronounced effect has been observed in weberites like Na_2NiMF_7[178,193] and its trigonal variety Na_2MnFeF_7.[180] In both cases the trans terminal bonds, though attached to tervalent M cations, are even longer than the bridging ones. They are affected as well by unusual short Na–F bonds on the opposite side (Figure 14).

Since for the calculation of bond valences the direction of a bond has no significance, in these cases of "trans effect" the bond valence sums of the anions (and if calculated by the method of Brown and Altermatt those of the cations as well) may deviate considerably, up to about 15%, from the ideal formal charge.

E. Electronic Effects

The structural influence of partially occupied d orbitals depends on the symmetry of both the orbitals and the ligand field. In transition-metal fluorine compounds octahedral ligand fields are predominant and lead with few exceptions to high-spin behavior. In all cases of "symmetrical" occupation of d orbitals like d^3, d^5, and d^8, no structural consequences are expected other than those already implied in the mean bond length. Indeed, the crystal structures of, for example, Cr^{3+} or Fe^{3+} fluorine compounds, are usually isotypic with the corresponding main-group compounds of say Al^{3+} and Ga^{3+} and reveal no special distortions which are not due to size effects. In the second- and third-row transition metals, however, the effect of π-back-bonding on the bridge angle M–F–M is discussed.[246,247]

1. Jahn–Teller Effect in Octahedral Fluorometalates

If the electron density distribution around a cation does not match the O_h symmetry of the ligand octahedron, degenerate ground states result which are instable in the sense of the Jahn–Teller theorem[248] and give rise to dynamic or static distortion. Generally there exist two different groups of Jahn–Teller-instable complex anions: The "weak" Jahn–Teller systems derive from triply degenerate T ground terms as present at d^1 (Ti^{3+}), d^2 (V^{3+}), d^6 (Fe^{2+}, Co^{3+}), or d^7 (Co^{2+}, Ni^{3+}) configurations. The "strong" Jahn–Teller systems derive from twofold degenerate E_g ground terms of d^4 (Cr^{2+}, Mn^{3+}), d^9 (Cu^{2+}), or d^7 low spin (Ni^{3+}).

In crystals vibronic coupling between electron motion and lattice modes may result in ferrodistortive or antiferrodistortive order of statically distorted ligand polyhedra; this is often called the cooperative Jahn–Teller effect. Recent surveys of the theory of the Jahn–Teller effect and numerous model compounds are given in ref 249 and 250.

The driving force to distort the ligand polyhedron is the anisotropic d-electron density. Therefore a weak effect is expected for T-term ions, where the unequally occupied t_{2g} orbitals are only weakly π-antibonding. For the Jahn–Teller ions with an E_g ground term the e_g orbitals with considerable σ-antibonding properties are unequally occupied and therefore should produce a strong effect.

Indeed, with few exceptions, in crystal structures of transition-metal fluorometallates Jahn–Teller-induced static distortions are only found for the strong Jahn–Teller ions Cr^{2+}, Mn^{3+}, Cu^{2+}, and Ni^{3+} (low spin). In three-dimensionally connected octahedra as well as in isolated MF_6 anions, a distortion which has no counterpart in a substituted non-Jahn–Teller ion may clearly be attributed to the electronic influence. In Table XI the effect of electron configuration on the geometry of the MF_6 octahedra and the relative bond valences are shown for the MF_2 rutiles.

The strong Jahn–Teller ions Cr^{2+} (d^4) and Cu^{2+} (d^9) display strongly elongated octahedra (d_{ax}/d_{eq} = 1.22 and 1.19, respectively), which is reflected in a weakening of the axial bonds by more than 50%. For the weak Jahn–Teller ions only in the case of Fe^{2+} (d^6 high spin) a comparatively small octahedral compression (d_{ax}/d_{eq} = 0.94) is observed, which is, however, significantly more pronounced than for the non-Jahn–Teller ions. As expected for the t_{2g}^4 e_g^2 configuration the corresponding additional weakening of the equatorial bonds (about 7%) is only small.

However, in "anisotropic" chain or layer structures an octahedral distortion is already produced by the low-dimensional bridging (see section C). Now the question arises as to what extent an additional electronic effect contributes to the distortion. Because of the normalizing mentioned in calculating relative bond valences v_r, both contributions, structural and electronic, may be separated when we compare the corresponding bond valences of related compounds containing "normal" and "Jahn–Teller" ions, respectively. In this way one may derive the dependence of the Jahn–Teller effect on structure type.[145] Fluorometallates are a rather suitable class of model compounds for such studies. For some compounds (especially those of the strong Jahn–Teller ion Mn^{3+}) structural data of all principal types of structural dimensionality are available and may be compared with the "normal-ion" structures (see also Table XII). The best reference compounds are the corresponding Fe(III) fluorides, because Fe^{3+} and Mn^{3+} have the same effective ionic radius.

2. Structure and Jahn–Teller Effect in Fluoromanganates(III)

a. Quasi-Isolated Octahedra. The only well-docu-

TABLE XII. Mean Bond Lengths (pm) and Relative Bond Valences in Compounds of "Strong" Jahn-Teller Ions As Compared with Related Non-Jahn-Teller Ions

structure type	compd	$d(M-F)_{ax}$	$d(M-F)_{eq}$	$v_{r(ax)}$	$v_{r(eq)}$	ref
isolated octahedra	K_2NaMnF_6	206	186	0.69	1.16	257
	Rb_2NaFeF_6	193.3	193.3	1	1	51
trans chains	Li_2MnF_5	212.3	184.7	0.59	1.205	97
	Cs_2MnF_5	211.4	185.6	0.61	1.19	96
	$Rb_2MnF_5 \cdot H_2O$	208.9	184.8	0.63	1.18	100
	$Rb_2AlF_5 \cdot H_2O$	188.7	178.3	0.82	1.09	90
cis chains	$BaMnF_5$	210.0	183.3	0.60	1.20	87
	$BaGaF_5$	193.4	185.7	0.86	1.07	84
layers	$KMnF_4$	212.3	185.7	0.60	1.20	145
	$KFeF_4$ II	196.8[a]	192.2[b]	0.92	1.04	137
	K_2CuF_4	223.8	192.4	0.51	1.25	156, 261
	K_2ZnF_4	202.6	202.9	1.006	0.997	147
3-dimensional	MnF_3	209	185	0.63	1.19	260
	FeF_3	192	192	1	1	263, 264
	$KCuF_3$	225	192.5	0.50	1.25	161, 162
	$KZnF_3$	202.3	202.3	1	1	265

[a] Mean d(Fe-F) within the layer. [b] Mean d(Fe-F) terminal and in layer.

mented case of a dynamic Jahn-Teller effect in a fluoromanganate(III) has been found in $Cr(NH_3)_6MnF_6$,[255,256] which crystallizes in the cubic rock salt type. At 120 K the compound undergoes a reversible phase transition to a monoclinic structure with statically distorted MnF_6 octahedra. If the elastic forces within the lattice are intensified by the use of smaller countercations, e.g., in the elpasolites A_2BMnF_6,[70,257-259] a lowering of the ideal cubic symmetry $Fm3m$ to the tetragonal subgroup $F4/mmm$ is observed even at room temperature. It is due to a ferrodistortive order of strongly elongated octahedra (Table XII).

b. Three-Dimensionally Connected Octahedra. Most of the trifluorides of the first transition-metal series crystallize in the ReO_3-related rhombohedral VF_3 type structure, displaying $\bar{3}m$ symmetry for the metal centers. As this symmetry does not lift the degeneracy of the ground state of Mn^{3+}, in MnF_3[261] a further symmetry reduction to a monoclinic subgroup takes place, leading to an antiferrodistortive order of elongated octahedra.

c. Layer Structures. The compression of the octahedra in $TlAlF_4$-related layer structures may be considerable (e.g., $d(M-F)_{ax}/d(M-F)_{eq} = 0.96$ in $CsFeF_4$[141]). Nevertheless, in the corresponding Mn(III) compounds $AMnF_4$ (A = K, Cs)[144,145] the Jahn-Teller effect does not assimilate to this compression or enhance it, though this would lift the degeneracy of the ground state as well. Rather, the octahedra become elongated and order in an antiferrodistortive way, the longest axes being oriented within the layers. Similar order patterns have been reported for layer compounds of the other strong Jahn-Teller ions Cu^{2+} (e.g., K_2CuF_4[156,261]) and Cr^{2+} (e.g., Rb_2CrCl_4[262]). The order of differently occupied e_g orbitals within the layers has remarkable consequences for the magnetic ordering. If the puckering of the layers is not too strong, two-dimensional ferromagnetism occurs in the cooperatively Jahn-Teller-ordered sheets;[144] this may be contrasted with, for example, $CsFeF_4$, in which two-dimensional antiferromagnetism is found.[141]

d. Linear-Chain Structures. In contrast to other fluorometallates(III), MnF_6^{3-} has a pronounced tendency to form linear-chain compounds with trans connection via vertices of the octahedra (see Table IV). In all the compounds A_2MnF_5 (A = Li, Na, Rb, NH_4, Cs),[93-97] $A_2MnF_5 \cdot H_2O$ (A = K, Rb, Cs),[96,98-100] and $AMnF_5 \cdot H_2O$ (A = Sr, Ba)[107] the octahedra are strongly elongated in the chain direction, much more than would be expected from the bridging effect only. The geometry of the octahedron itself is nearly independent on the bridge angle Mn-F-Mn, which increases with the size of the countercation from 121.5° in Li_2MnF_5 to 180° in Cs_2MnF_5. The only cis-connected chain of MnF_6 octahedra has been found in $BaMnF_5$,[87] where elongated octahedral axes are ordered antiferrodistortively in the plane of the cis connection.

3. Dependence of Jahn-Teller Effect on Structure Types

The relative bond valence calculations performed for fluoromanganates(III) are compiled in Table XII. They yield as the most important result that the degree of octahedral distortion is nearly independent of the structure type. Only the isolated octahedra in the elpasolite K_2NaMnF_6 show a smaller effect. Obviously, the weak elastic coupling between the isolated octahedra reduces the cooperative Jahn-Teller effect by about $^1/_4$ with respect to the structures with connected octahedra.

In these one-, two-, and three-dimensional systems a nearly constant weakening of about 40% results for the relative bond valences of the long axes, $v_{r(ax)}$. Comparison with the non-Jahn-Teller compounds reveals that in the linear-chain structures about half of this total bond weakening must be ascribed to the structural bridging effect. The remaining 20% are made by the electronic effect. There is no difference between a trans and a cis chain.

In layer structures, the pure bridging contribution to the bond weakening within the layers is comparatively small. The strong elongation of the octahedra in an antiferrodistortively ordered sheet with total axial bond weakening of again 40% is due in the greatest part (about $^4/_5$) to the Jahn-Teller effect. The corresponding strengthening of the four equatorial bonds, $v_{r(eq)}$, two of which also oriented within the layer, cooperatively compensates for this.

In the case of the three-dimensionally connected octahedra, as in MnF_3 or the perovskite $KCuF_3$, of course the total distortion effect is caused electronically.

The strong Jahn-Teller ions Cu^{2+} and Cr^{2+}, as the examples in Tables XI and XII show, exhibit still stronger distortions of their MF_6 octahedra than Mn^{3+} does. This is to be expected, as the approximately

constant electronic effect becomes relatively more pronounced when the Coulombic forces within the M–F bonds are weaker.

The interesting feature, viz., that the electronic Jahn–Teller distortion decreases with the increasing extent of structural distortion so as to keep the total distortion approximately constant, may provide some explanation for the unusual stability and high tendency of formation of chain structure fluoromanganates(III). Owing to the nearly constant degree of octahedral distortion in all structure types, the electronic stabilization energy $2\delta_1$ (6000–7700 cm^{-1} from ligand field spectra[250]) remains approximately the same. This energy gain is, in part, offset by the loss of Coulombic energy in the distorted octahedra: the decrease of Coulombic energy when lengthening the axial bonds is not completely compensated for by a shortening of the equatorial bonds, because repulsion forces rapidly increase. If we compare the relative stabilities of the Jahn–Teller systems with a related non-Jahn–Teller compound, only the electronic part of the bond weakening and the corresponding loss of Coulombic energy has to be taken into account. This amount is by far least for the chain compounds and largest for the zero- and three-dimensionally-connected structures. The easy precipitation of ternary trans chain Mn(III) fluorides from HF solution simply on addition of alkali-metal or even alkaline-earth fluorides may thus be better understood, as well as the fact that hydrates also form those chain structures. By contrast, in "normal" fluorometallates(III) the formation of cryolites is favored under these conditions. Again, the trifluorides of Cr, V, and Fe are very stable compounds, but MnF_3 is highly sensitive to hydrolysis.

V. Hydrogen Bonds in Fluorides

The lone electron pairs of fluoride ions may act as powerful acceptors (A) for acid hydrogen atoms of suitable donor groups (D–H). Thus a variety of fluorine compounds containing such donors is known, where hydrogen bonds of different strength play an important role in the three-dimensional linking of the crystal structures. The most common donor groups are the N–H groups, mostly from ammonium ions, the O–H groups from H_2O or hydroxide groups, and the H–F molecules in bifluorides. In contrast to the dominant but undirected Coulombic interactions within an ionic solid, the hydrogen bonds favoring linear arrays D–H···A now introduce a directed bonding contribution. Below we give a short survey of the principal structural features within these three groups of hydrogen bond systems.

Most geometric data of hydrogen bonds still stem from X-ray diffraction studies and the hydrogen atom positions are therefore not very precise. Hence we will discuss mainly the donor–acceptor distances D···A as a rough measure of the relative strength of a hydrogen bond.

A. Hydrogen Bonds between Ammonium and Fluoride Ions

Owing to its tetrahedral geometry the ammonium ion is able to form up to four hydrogen bonds, provided the surrounding acceptors match this tetrahedral symmetry approximately. Thus the gain of hydrogen bond energy is responsible for the unusual tetrahedral coordination sometimes found for the ammonium ion, which in fluorides is as large as the rubidium ion (cf. Table V; the effective size of NH_4^+ has been treated in detail by Knop et al.[175]). In spite of this, NH_4F crystallizes in the wurtzite type rather than in the rock salt or CsCl type structure. The low CN 4 for ammonium seems to be tied to the presence of "independent" fluoride ions which are the acceptors in all the CN 4 examples of Table XIII, where the N···F distances are listed for different coordinations of the ammonium ion.

TABLE XIII. Ammonium Ions Coordinated by Fluoride

compd	N···F, pm	ref
	CN = 4	
NH_4F	271	266
NH_4HF_2	271	267
$(NH_4)_2[Cr(H_2O)_6]F_5$	272	268, 269
$NH_4CuTiF_7 \cdot 4H_2O$	278	270
	CN = 6	
$Cs_2NH_4FeF_6$	268	271
$(NH_4)_3FeF_6$	264	272
	CN = 8	
NH_4AlF_4	290	129
	CN = 12	
NH_4MnF_3	300	273
$(NH_4)_2SiF_6$	300	274
$(NH_4)_2NaFeF_6$	301	145
$(NH_4)_3FeF_6$	324	272

In sites of higher coordination, of course, the number of possible acceptor atoms is higher than the number of donor hydrogen atoms. Thus, depending on the temperature, one observes dynamic rotation, orientational disorder or, below a phase transition point, fixed orientation of the ammonium ions with respect to the fluorine environment. The hydrogen bonds may then be bi- or even trifurcated. Interesting order/disorder phase transitions have been found, for example, in ammonium perovskites NH_4MF_3,[275a] cryolites $(NH_4)_3MF_6$,[145,272,276-279] and the elpasolites $(NH_4)_2NaFeF_6$[280] and $Cs_2NH_4FeF_6$.[145,277]

A suitable method for revealing the presence of hydrogen bonding in such cases is IR and Raman spectroscopy, especially using the isotopic probe ion NH_3D^+ in partially deuteriated ammonium compounds. For details we refer to the work of Knop et al.[277] Strong hydrogen bonds N–H···F occur mainly at the low CN 4 with a typical N···F distance of 272 pm. For ammonium ions in the 6-coordinated sites of the cryolites or elpasolites the N···F distances are even shorter (about 264 pm). This is obviously a consequence of the mismatch of the octahedral surrounding and the tetrahedral symmetry of the ammonium group. It is therefore not surprising that in such cases the spectroscopic evidence points to a very complicated and varied hydrogen bond behavior.[277,281] Only weak hydrogen bonds are found for CN 12. The reason is probably that the cuboctahedral 12-coordinated site (e.g., in the cryolites) exhibits a N···F distance of 300 pm or more, too large for the formation of strong hydrogen bonds. Because of the orientational disorder of the ammonium ions the cryolites $(NH_4)_3MF_6$ of the first-row transition metals all are cubic at room temperature, while the corresponding compounds A_3MF_6 of the large alkali-metal ions (A = K, Rb, Cs) have complicated pseudotetragonal superstructures, as mentioned earlier.

TABLE XIV. Selected Compounds with O–H• • •F Hydrogen Bridges

compd		O···F, pm	ref
1. Complex Fluoride/Complex Water			
$CuF_2·2H_2O$		272	283
$FeF_2·4H_2O$		260	284
$FeF_3·3H_2O$ II		258	285
$CdGaF_5·7H_2O$		270	282
$RbMnF_4·H_2O$		274	286
$RbVF_4·2H_2O$		257	282
$CuZrF_6·4H_2O$		265	287
$CuBeF_4·5H_2O$		272	288
$(NH_4)_2Co(H_2O)_6(BeF_4)_2$		269	289
$Fe(H_2O)_6SiF_6$		270	290
$Cu_3M_2F_{12}·12H_2O$ (M = V, Cr, Fe)		270	127, 179a
$Cu(H_2O)_4SiF_6$		272	291
2. Complex Fluoride/Crystal Water			
$FeF_3·3H_2O$ II		270	285
$Rb_2AlF_5·H_2O$		273	90
$K_2MnF_5·H_2O$		274	98
$Cs_2MnF_5·H_2O$		274	99
$SrMnF_5·H_2O$		282	107
$Li_2SnF_6·2H_2O$		298	292
$Li_2TiF_6·2H_2O$		305	292
3. "Free" Fluoride/Complex Water			
$[Cr(H_2O)_6]F_3·3H_2O$		262	293
$(NH_4)_2[Cr(H_2O)_6]F_5$		254	268, 269
$NH_4CuTiF_7·4H_2O$		252	270
4. "Free" Fluoride/Crystal Water			
$KF·2H_2O$	3-dimen	270	294
$KF·4H_2O$	3-dimen	274	295
$Te(OH)_6·2CsF·2H_2O$	4-ring	268	296
$Ba_4Fe_3F_{17}·3H_2O$	4-ring	265	201
$[Cr(H_2O)_6]F_3·3H_2O$	6-ring	264	293
$(CH_3)_4NF·4H_2O$	3-dimen[a]	263	297
$[(C_2H_5)_4NF]_4·11H_2O$	3-dimen	270	298

[a] Water tricoordinated.

B. Hydrogen Bonds between Water and Fluorine Species

Most of the bi- and tervalent metal cations are able to form octahedral complexes with water molecules as ligands as well as with fluoride ions. On the other hand, fluorometallates often contain crystal water, and in some cases "independent" fluoride anions are present in a structure. As will be shown, the geometry and strength of hydrogen bonds depend on the bonding state of both the donor and the acceptor. Thus it seems useful to subdivide the compounds containing O–H···F hydrogen bonds according to the bonding type of their constituents.

1. Water and Fluorine Both Are Complex Ligands

To this group[145,282] belong mainly some mixed-ligand compounds like $FeF_2·4H_2O$ (=$Fe(H_2O)_4F_2$) and heterometallic systems with a $(M(H_2O)_6)^{2+}$ cation and the anions $(MF_5H_2O)^{2-}$ or $(SiF_6)^{2-}$. In the latter compounds the three-dimensional linking within the structure is effected by a hydrogen bond network instead by the alkali-metal or alkaline-earth cations in anhydrous fluorides. A kind of anti-perovskite arrangement is present in the compounds $Cu_3M_2F_{12}·12H_2O$, which may be described as $[MF_6^{3-}][MF_6^{3-}][(Cu(H_2O)_4^{2+}]_3$.[127,179,179a] The mean O···F distance in all these compounds is 269 pm.

The coordinative bonding of the donor H_2O molecules as well as of the acceptor fluoride ions reduces the number of possible H bonds: The H_2O ligand is only able to use two donor functions, whereas its two acceptor lone pairs are engaged in coordination to the metal center. Thus the H_2O molecule is generally tricoordinated and the two acceptor fluorine atoms preferably lie within the M–OH_2 plane, but other geometries, such as bifurcated H bonds, are also known. An exception from this rule is found, for example, if the coordinative M–OH_2 bond is weakened by a strong Jahn–Teller effect: in $Na[MnF_4(H_2O)_2]·H_2O$[299] the aquo ligands are tetragonally coordinated. One of the two crystallographically independent H_2O ligands of the $[MnF_4(H_2O)_2]^-$ anion (d(Mn–O) = 224.6 pm) is involved in three H bonds, two donor O–H···F bonds and one acceptor O···H–O bond from the crystal water molecule (Figure 15).

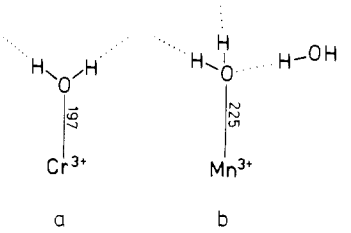

Figure 15. Geometry of hydrogen bonding at metal-coordinated aquo ligands. (a) "Normal" case: trigonal coordination. (b) In $Na[MnF_4(H_2O)_2]·H_2O$: tetrahedral coordination.

Similarly, the fluorine ligands in an octahedral complex anion are restricted in the use of their acceptor functions and thus only in rare cases[179a] more than two H bonds are formed.

2. Complex Fluoro Anions and Crystal Water

The hydrogen bonds between metal-coordinated fluorine atoms and "free" crystal water show somewhat larger average O···F distances, of about 279 pm, than in the previous group of compounds. Sporadically, much larger distances are observed in both groups. This may be understood by taking into account packing requirements for the aquo ligands, e.g., in the inverse weberites like $Fe_2F_5·2H_2O$[181–183] or in the related compound $Fe_3F_8·2H_2O$.[300] On the other hand, the "free" molecules of crystal water are still weakly bonded. All varieties between coordination to the alkali-metal or alkaline-earth countercations and a mere space-filling function have been observed. Examples of very weakly bonded "zeolitic" water are the pyrochlore $KNiCrF_6·H_2O$[170] (d(O···F) = 330 pm) or the HTB structure compound $(H_2O)_{0.33}FeF_3$[169] (d(O···F) = 309 pm).

In the Jahn–Teller-stabilized trans-chain compounds $A_2MnF_5·H_2O$ (A = Rb, Cs)[94,96] a reversible topotactical dehydration to the anhydrous trans-chain compounds has been observed. In the case of the isotypic "normal" ion compounds $Rb_2AlF_5·H_2O$ and $Rb_2FeF_5·H_2O$,[90] however, dehydration is irreversible. The aluminum compound decomposes into $RbAlF_4$ and Rb_3AlF_6. $Rb_2FeF_5·H_2O$ transforms into the anhydrous fluoride (Rb_2FeF_5) with cis-chain structure. Obviously, trans-chain structures are formed with "normal" ions only if hydrogen bonds stabilize them.

3. Aquo Complexes and "Independent" Fluoride Anions

The existence of noncoordinated fluoride ions in the presence of complex aquo cations in a structure is very

TABLE XV. F• • •F Hydrogen Bond Distances (pm) in Bifluorides with Corrections for Thermal Motion

compd	F···F	F···F_{cor}	ref
$NaHF_2$	226.4	228.8	304
KHF_2	227.7	229.3	304
NH_4HF_2	226.9	229.1	304
	227.5	229.7	
$BaF(HF_2)$	227.0	228.1	305
$SrF(HF_2)$	226.7	227.1	305

unusual, because in solution most metal cations rapidly and irreversibly exchange H_2O against fluoride ligands. Therefore, in contrast to complexes with chloride or sulfate ligands, no hydrate isomerism is known in fluoride hydrates. There are only two types of compounds where hexaquo cations coexist in a crystal with noncoordinated fluoride anions:

In the red chromium(III) fluoride hydrates $[Cr(H_2O)_6]F_3$[272] and $[Cr(H_2O)_6]F_3 \cdot 3H_2O$[293] as well as in $(NH_4)_2[Cr(H_2O)_6]F_5$[268] retention of the unchanged hexaquo cations during precipitation of the compounds from HF solution is possible, owing to the extreme slow ligand exchange rate of hexaquochromium(III) cations. The half-time is about 50 h for Cr^{3+} but in the range of 10^{-3} s for the other common bi- and tervalent metal ions.[301]

The other group belonging to this type of hydrogen bonding, $M-OH_2\cdots F$, are the compounds $NH_4CuMF_7 \cdot 4H_2O$ (M = Ti (crystal structure determined), Si, and Sn).[270] On the one hand, the aquo complex of Cu(II) is rather stable. On the other hand, an additional stabilization of the "free" fluoride anion is provided by the H bonds from the ammonium ions.

The mean O···F distance of 256 pm in this group is the shortest of all types of HO–H···F bridges, except that found in the adduct $HF \cdot H_2O$[302] (mean O···F = 246.6 pm). However, the latter compound, which melts at −36 °C, belongs to the oxonium salts, where the H_3O^+ groups act as very strong donors. The structure consists of a puckered two-dimensional honeycomb-like hydrogen bond network.

4. Crystal Water and "Independent" Fluoride Anions

There are some compounds containing "free" fluoride anions and molecules of crystal water which form together four- or six-membered rings or three-dimensional networks (Table XIV). Generally both water molecules and fluoride centers adopt tetrahedral coordination and use all their donor and acceptor functions. To this class of hydrogen bond compounds belong, for example, the hydrates of potassium fluoride or clathrates like $(CH_3)_4NF \cdot 4H_2O$ or $[(C_2H_5)_4NF]_4 \cdot 11H_2O$. The mean O···F distance of 268 pm is again higher than in the previous class.

5. Hydrogen Bond Lengths and the Bonding State of Donor and Acceptor Groups

Comparison of the mean O···F hydrogen bond lengths exhibited by the above four classes of fluoride hydrates clearly reveals the following trend: if the donor water molecules are engaged in an aquo complex, the hydrogen bond is strengthened, but engagement of the acceptor fluorine atoms in a complex anion weakens it. Thus the weakest hydrogen bonds are found in fluorometallates containing "free" crystal water (mean O···F = 279 pm) and the strongest ones in the rare aquo complexes with "free" fluoride anions (mean O···F = 256 pm). The combinations where either both parts are complex ligands or both are "free" are intermediate in strength and show approximately the same medium mean O···F distance of 269 and 268 pm, respectively.

This behavior is in accordance with expectation, if criteria for the strength of hydrogen bonds are used such as those arising, for example, from the theoretical investigations of Allen.[303] Thus the strength of a hydrogen bond D–H···A increases with an increasing dipole moment of the D–H function and with the increasing extension of the lone electron pair at the acceptor A. Undoubtedly the polarity of the O–H bond will rise if the lone electron pairs of a water molecule are engaged by complexation to a metal cation. On the other hand, a quasi-free fluoride anion with its high effective negative charge will certainly have the largest extension of its electron pairs. So the observed gradation of hydrogen bond lengths seems quite reasonable.

C. Hydrogen Bonds in Bifluorides

The strongest hydrogen bonds are observed in the bifluoride anions of compounds AHF_2 (A = Li, Na, K, Rb, NH_4, Cs) and $AF(HF_2)$ (A = Sr. Ba). The F···F distances claimed from X-ray investigations (Table XV) are approximately the same for all compounds, though in the alkaline-earth compounds a slightly asymmetrical H bridge is likely, whereas in the alkali-metal compounds symmetrical H bonds are found. Strongly asymmetric H bonds are observed in solid HF[306] (F–H···F = 249 pm), while oxonium bifluoride H_3OHF_2[302] shows an intermediate behavior (F–H···F = 236.7 pm) similar to that found in KH_2F_3.[307]

Acknowledgments. We thank Professor O. Knop, Halifax (Canada), for helpful discussions and for reading the manuscript. The financial support of our work by the Deutsche Forschungsgemeinschaft and the Fonds der Chemischen Industrie is gratefully acknowledged.

References

(1) Pauling, L. *J. Am. Chem. Soc.* **1929**, *51*, 1010.
(2) Wells, A. F. *Structural Inorganic Chemistry*, 5th ed.; Clarendon Press: Oxford, 1984.
(3) Banks, R. E.; Sharp, D. W. A.; Tatlow, J. C., Eds. *J. Fluorine Chem.* **1986**, *33*, 1–399.
(4) Hagenmuller, P., Ed. *Inorganic Solid Fluorides. Chemistry and Physics*; Academic Press: New York, 1985.
(5) Babel, D. *Struct. Bonding (Berlin)* **1967**, *3*, 1.
(6) Pies, W.; Weiss, A., Eds. *Landolt-Börnstein Tables, New Series*, 1973, Group III, Vol. 7, a and g.
(7) Penneman, R. A.; Ryan, R.; Rosenzweig, A. *Struct. Bonding (Berlin)* **1973**, *13*, 1.
(8) Greis, O.; Haschke, J. M. *Handb. Phys. Chem. Rare Earths* **1982**, *5*, 387.
(9) Edwards, A. J. *Adv. Inorg. Chem. Radiochem.* **1982**, *27*, 83.
(10) Babel, D.; Tressaud, A. *Inorganic Solid Fluorides*; Hagenmuller, P., Ed.; Academic Press: New York, 1985; p 77.
(11) Schnering, H. G. v.; Kolloch, B.; Kolodziejczyk, A. *Angew. Chem.* **1971**, *83*, 440.
(12) Odenthal, R. H.; Hoppe, R. *Z. Anorg. Allg. Chem.* **1971**, *385*, 92.
(13) Edwards, A. J.; Jones, G. R. *J. Chem. Soc. A* **1969**, 1936.
(14) Hoppe, R.; Homann, R. *Z. Anorg. Allg. Chem.* **1970**, *379*, 193.
(15) Mueller, B. G. *J. Fluorine Chem.* **1982**, *20*, 291.
(16) Mueller, B. G. *Z. Anorg. allg. Chem.* **1982**, *491*, 245.
(17) Schnering, H. G. v.; Vu, D.; Peters, K. *Z. Kristallogr.* **1983**, *165*, 305.
(18) Schnering, H. G. v. *Z. Anorg. Allg. Chem.* **1967**, *353*, 13.
(19) Burns, J. H. *Acta Crystallogr.* **1962**, *15*, 1098.
(20) Teufer; G. *Acta Crystallogr.* **1956**, *9*, 539.
(21) Bode, H.; Döhren, H. v. *Acta Crystallogr.* **1958**, *11*, 80.
(22) Gabuda, S. P.; Kozlova, S. G.; Kriger, Y. G.; Goncharuk, V. K. *J. Struct. Chem. (Engl. Transl.)* **1986**, *27*, 221.

(23) Hepworth, M. A.; Jack, K. H.; Westland, G. J. *J. Inorg. Nucl. Chem.* **1956**, *2*, 79.
(24) Hoskins, B. F.; Linden, A.; Mulvaney, P. C.; O'Donnell, T. A. *Inorg. Chim. Acta* **1984**, *88*, 217.
(25) Hoard, J. L.; Vincent, W. B. *J. Am. Chem. Soc.* **1940**, *62*, 3126.
(26) Mueller, B. G.; Hoppe, R. *Z. Anorg. Allg. Chem.* **1983**, *498*, 128.
(27) Hoppe, R.; Dähne, W. *Naturwissenschaften* **1960**, *47*, 397.
(28) deBournonville, M. B.; Bizot, D.; Chassaing, J.; Quarton, M. *J. Solid State Chem.* **1986**, *62*, 212.
(29) Zalkin, A.; Forrester, J. D.; Templeton, D. H. *Acta Crystallogr.* **1964**, *17*, 1408.
(30) Schaefer, G. F. *Z. Kristallogr.* **1986**, *175*, 269.
(31) Hebecker, C.; Schnering, H. G. v.; Hoppe, R. *Naturwissenschaften* **1966**, *53*, 154.
(32) Hoard, J. L.; Vincent, W. B. *J. Am. Chem. Soc.* **1939**, *61*, 2849.
(33) Bode, H.; Wendt, W. *Z. Anorg. Allg. Chem.* **1952**, *269*, 165.
(34) Loehlin, J. H. *Acta Crystallogr., Sect. C* **1984**, *C40*, 570.
(35) Viebahn, W. *Z. Anorg. Allg. Chem.* **1971**, *386*, 335.
(36) Fleischer, T.; Hoppe, R. *Z. Naturforsch., B* **1982**, *37b*, 981.
(37) Babel, D. *Z. Anorg. Allg. Chem.* **1974**, *406*, 23.
(38) Burns, J. H.; Tennissen, A. C.; Brunton, G. D. *Acta Crystallogr., Sect. B* **1968**, *B24*, 225.
(39) Massa, W. *Z. Kristallogr.* **1980**, *153*, 201.
(40) Náray-Szabó, S. V.; Sasvári, K. *Z. Kristallogr.* **1938**, *99*, 27.
(41) Hawthorne, F. C.; Ferguson, R. B. *Can. Mineral.* **1975**, *13*, 377.
(42) Matvienko, E. N.; Iakubovich, O. V.; Simonov, M. A.; Ivashchenko, A. N.; Melnikov, O. K.; Belov, N. V. *Dokl. Akad. Nauk SSSR* **1981**, *257*, 105.
(43) Bode, H.; Teufer, G. *Z. Anorg. Allg. Chem.* **1975**, *290*, 1.
(44) Toth, L. M.; Brunton, G. D.; Smith, G. P. *Inorg. Chem.* **1969**, *8*, 2694.
(45) Tun, Z.; Brown, I. D.; Ummat, P. K. *Acta Crystallogr., Sect. C* **1984**, *40*, 1301.
(46) Brown, I. D.; Gillespie, R. J.; Morgan, K. R.; Tun, Z.; Ummat, P. K. *Inorg. Chem.* **1984**, *23*, 4506.
(47) Geller, S. *Am. Mineral.* **1971**, *56*, 18.
(48) Massa, W.; Post, B.; Babel, D. *Z. Kristallogr.* **1982**, *158*, 299.
(49) Morss, L. R. *J. Inorg. Nucl. Chem.* **1974**, *36*, 3876.
(50) Iakubovich, O. V.; Simonov, M. A.; Melnikov, O. K.; Urusov, V. S. *Dokl. Akad. Nauk SSSR* **1986**, *287*, 126.
(51) Massa, W.; Babel, D.; Epple, M.; Rüdorff, W. *Rev. Chim. Miner.* **1986**, *23*, 508.
(52) Winkler, H. G. F. *Acta Crystallogr.* **1954**, *7*, 33.
(53) Tressaud, A.; Darriet, J.; Lagassie, P.; Grannec, J.; Hagenmuller, P. *Mater. Res. Bull.* **1984**, *19*, 983.
(54) Babel, D.; Haegele, R. *J. Solid State Chem.* **1976**, *18*, 39.
(55) Golovastikov, N. I.; Belov, N. V. *Kristallografiya* **1978**, *23*, 42.
(56) Massa, W.; Babel, D. *Z. Anorg. Allg. Chem.* **1980**, *469*, 75.
(57) Domesle, R.; Hoppe, R. *Z. Kristallogr.* **1980**, *153*, 317.
(58) Domesle, R.; Hoppe, R. *Z. Anorg. Allg. Chem.* **1983**, *501*, 102.
(59) Holler, H.; Babel, D. *Z. Anorg. Allg. Chem.* **1985**, *523*, 89.
(60) Haegele, R. Thesis, Marburg, 1974.
(61) Alter, E.; Hoppe, R. *Z. Anorg. Allg. Chem.* **1974**, *405*, 167.
(62) Goldschmidt, V. M. *Naturwissenschaften* **1926**, *21*, 481.
(63) Babel, D.; Haegele, R.; Pausewang, G.; Wall, F. *Mater. Res. Bull.* **1973**, *8*, 1371.
(64) Shannon, R. D. *Acta Crystallogr., Sect. A* **1976**, *A32*, 751.
(65) Waddington, T. C. *Trans. Faraday Soc.* **1966**, *62*, 1482.
(66) Babel, D.; Massa, W.; Herdtweck, E. 9th European Crystallographic Meeting, Torino, Sept 1985.
(67) Babel, D.; Binder, F. *Z. Anorg. Allg. Chem.* **1983**, *505*, 153.
(68) Setter, J.; Hoppe, R. *Z. Anorg. Allg. Chem.* **1976**, *423*, 133.
(69) Alter, E.; Hoppe, R. *Z. Anorg. Allg. Chem.* **1974**, *407*, 313.
(70) Siebert, G.; Hoppe, R. *Z. Anorg. Allg. Chem.* **1972**, *391*, 117.
(71) Alter, E.; Hoppe, R. *Z. Anorg. Allg. Chem.* **1974**, *407*, 305.
(72) Alter, E.; Hoppe, R. *Z. Anorg. Allg. Chem.* **1975**, *412*, 110.
(73) Hoppe, W.; Hoppe, R. *Z. Anorg. Allg. Chem.* **1975**, *414*, 91.
(74) Weissenhorn, F. J. Thesis, Tübingen, 1972.
(75) Alter, E.; Hoppe, R. *Z. Anorg. Allg. Chem.* **1974**, *403*, 127.
(76) Hoppe, R.; Lehr, K. *Z. Anorg. Allg. Chem.* **1975**, *416*, 240.
(77) Arndt, J.; Babel, D.; Haegele, R.; Rombach, N. *Z. Anorg. Allg. Chem.* **1975**, *418*, 193.
(78) Herdtweck, E.; Massa, W.; Babel, D. *Z. Anorg. Allg. Chem.* **1986**, *539*, 87.
(79) Kissel, D.; Hoppe, R. *Z. Anorg. Allg. Chem.* **1986**, *532*, 17. (a) Liebau, F. *Structural Chemistry of Silicates: Structure, Bonding and Classification*; Springer: Berlin, Heidelberg, New York, Tokyo, 1985. (b) Hawthorne, F. C. *Am. Mineral.* **1985**, *70*, 455.
(80) Vlasse, M.; Matejka, G.; Tressaud, A.; Wanklyn, B. M. *Acta Crystallogr., Sect. B* **1977**, *B33*, 3377.
(81) Jacoboni, C.; DePape, R.; Poulain, M.; le Marouille, J. Y.; Grandjean, D. *Acta Crystallogr., Sect. B* **1974**, *B30*, 2688.
(82) Tressaud, A.; Soubeyroux, J. L.; Dance, J. M.; Sabatier, R.; Hagenmuller, P.; Wanklyn, B. M. *Solid State Commun.* **1981**, *37*, 479.
(83) von der Muehll, R.; Daut, F.; Ravez, J. *J. Solid State Chem.* **1973**, *8*, 206.
(84) Domesle, R.; Hoppe, R. *Rev. Chim. Miner.* **1978**, *15*, 439.
(85) Domesle, R.; Hoppe, R. *Z. Anorg. Allg. Chem.* **1982**, *495*, 16.
(86) Holler, H.; Kurtz, W.; Babel, D.; Knop, W. *Z. Naturforsch., B* **1982**, *37b*, 54.
(87) Bukovec, P.; Hoppe, R. *Z. Anorg. Allg. Chem.* **1984**, *509*, 138.
(88) Abjean, P.; Leblanc, M.; DePape, R.; Ferey, G.; Nowogrocki, G. *Acta Crystallogr., Sect. C* **1985**, *C41*, 1696.
(89) Brosset, C. *Z. Anorg. Allg. Chem.* **1937**, *235*, 139.
(90) Fourquet, J. L.; Plet, F.; DePape, R. *Rev. Chim. Miner.* **1981**, *18*, 19.
(91) Fourquet, J. L.; Plet, F.; DePape, R. *Acta Crystallogr., Sect. B* **1981**, *B37*, 2136.
(92) Courant, E.; Fourquet, J. L.; DePape, R. *J. Solid State Chem.* **1985**, *60*, 343.
(93) Sears, D. R.; Hoard, J. L. *J. Chem. Phys.* **1969**, *50*, 1066.
(94) Guenter, J. R.; Matthieu, J. P.; Oswald, H. R. *Helv. Chim. Acta* **1978**, *61*, 328.
(95) Massa, W. *Acta Crystallogr., Sect. C* **1986**, *C42*, 644.
(96) Hahn, F. Diplomarbeit, Marburg, 1985.
(97) Pebler, J.; Massa, W.; Lass, H.; Ziegler, B. *J. Solid State Chem.* **1987**, *71*, 87.
(98) Edwards, A. J. *J. Chem. Soc. A* **1971**, 2653.
(99) Kaučič, V.; Bukovec, P. *Acta Crystallogr., Sect. B* **1978**, *B34*, 3337.
(100) Bukovec, P.; Kaučič, V. *Acta Crystallogr., Sect. B* **1978**, *B34*, 3339.
(101) Dumora, D.; von der Muehll, R.; Ravez, J. *Mater. Res. Bull.* **1971**, *6*, 561.
(102) Wu, K. K.; Brown, I. D. *Mater. Res. Bull.* **1973**, *8*, 593.
(103) Eicher, S. M.; Greedan, J. E. *J. Solid State Chem.* **1984**, *52*, 12.
(104) Wandner, K. H.; Hoppe, R. *Rev. Chim. Miner.* **1986**, *23*, 520.
(105) von der Muehll, R.; Ravez, J. *Rev. Chim. Miner.* **1974**, *11*, 652.
(106) von der Muehll, R.; Andersson, S.; Galy, J. *Acta Crystallogr., Sect. B* **1971**, *B27*, 2345.
(107) Massa, W.; Burk, V. *Z. Anorg. Allg. Chem.* **1984**, *516*, 119.
(108) Vlasse, M.; Chaminade, J. P.; Dance, J. M.; Saux, M.; Hagenmuller, P. *J. Solid State Chem.* **1982**, *41*, 272.
(109) Ferey, G.; Leblanc, M.; DeKozak, A.; Samouel, M.; Pannetier, J. *J. Solid State Chem.* **1985**, *56*, 288.
(110) Fleischer, T.; Hoppe, R. *Z. Anorg. Allg. Chem.* **1982**, *493*, 59.
(111) DeKozak, A.; Leblanc, M.; Samouel, M.; Ferey, G.; DePape, R. *Rev. Chim. Miner.* **1981**, *18*, 659.
(112) Dewan, J. C.; Edwards, A. J. *J. Chem. Soc., Chem. Commun.* **1977**, *15*, 533.
(113) Dewan, J. C.; Edwards, A. J.; Guy, J. J. *J. Chem. Soc., Dalton Trans.* **1986**, 2623.
(114) Babel, D.; Knoke, G. *Z. Anorg. Allg. Chem.* **1978**, *442*, 151.
(115) Loesch, R.; Hebecker, C. *Z. Naturforsch., B* **1979**, *34b*, 131.
(116) Fourquet, J. L.; Plet, F.; Courbion, G.; Balou, A.; DePape, R. *Rev. Chim. Miner.* **1979**, *16*, 490.
(117) Domesle, R.; Hoppe, R. *Z. Anorg. Allg. Chem.* **1982**, *495*, 27.
(118) Fourquet, J. L.; Plet, F.; DePape, R. *Acta Crystallogr., Sect. B* **1980**, *B36*, 1997.
(119) Courbion, G.; Jacoboni, C.; DePape, R. *Acta Crystallogr., Sect. B* **1976**, *B32*, 3190.
(120) Knoke, G.; Verscharen, W.; Babel, D. *J. Chem. Res. (S)* **1979**, 213.
(121) Dance, J. M.; Tressaud, A.; Massa, W.; Babel, D. *J. Chem. Res. (S)* **1981**, 202.
(122) Schnering, H. G. v.; Bleckmann, P. *Naturwissenschaften* **1968**, *55*, 342.
(123) Keve, E. T.; Abrahams, S. C.; Bernstein, J. L. *J. Chem. Phys.* **1969**, *51*, 4928.
(124) Keve, E. T.; Abrahams, S. C.; Bernstein, J. L. *J. Chem. Phys.* **1970**, *53*, 3279.
(125) Sciau, P.; Grebille, D.; Berar, J. F.; Lapasset, J. *Mater. Res. Bull.* **1986**, *21*, 843.
(126) Babel, D.; Herdtweck, E.; Holler, H.; Schmidt, R. E.; Kummer, S. *J. Fluorine Chem.* **1985**, *29*, 37.
(127) Kummer, S. Thesis, Marburg, 1986.
(128) Launay, J. M.; Bulou, A.; Hewat, A. W.; Gibaud, A.; Laval, J. Y.; Nouet, J. *J. Phys. (Paris)* **1985**, *46*, 771.
(129) Bulou, A.; Leblé, A.; Hewat, A. W.; Fourquet, J. L. *Mater. Res. Bull.* **1982**, *17*, 391.
(130) Leblanc, M.; Ferey, G.; DePape, R.; Teillet, J. *Acta Crystallogr., Sect. C* **1985**, *C41*, 657.
(131) White, M. A.; Wagner, B. D. *J. Chem. Phys.* **1985**, *83*, 5844.
(132) Jouanneaux, A.; Leblé, A.; Fayet, J. C.; Fourquet, J. L. *Europhys. Lett.* **1987**, *3*, 61.
(133) Omaly, J.; Batail, P.; Grandjean, D.; Avignant, D.; Cousseins, J. C. *Acta Crystallogr., Sect. B* **1976**, *B32*, 2106.
(134) Heger, G.; Geller, R.; Babel, D. *Solid State Commun.* **1971**, *9*, 335.
(135) Sabatier, R.; Charroin, G.; Avignant, D.; Cousseins, J. C.; Chevalier, R. *Acta Crystallogr., Sect. B* **1979**, *B35*, 1333.

(136) Saint-Gregoire, P.; Perez, A.; Almairac, B.; Lopez, M. *Phys. Status Solidi A* **1985**, *87*, K1.
(137) Lapasset, J.; Sciau, P.; Moret, J.; Gros, N. *Acta Crystallogr., Sect. B* **1986**, *B42*, 258; **1987**, *B43*, 111.
(138) Tressaud, A.; Galy, J.; Portier, J. *Bull. Soc. Fr. Mineral. Cristallogr.* **1969**, *92*, 335.
(139) Deblieck, R.; Van Landuyt, J.; Amelinckx, S. *J. Solid State Chem.* **1985**, *59*, 379.
(140) Hidaka, M.; Akiyama, H.; Wanklyn, B. M. *Phys. Status Solidi A* **1986**, *97*, 387.
(141) Babel, D.; Wall, F.; Heger, G. *Z. Naturforsch., B* **1974**, *29b*, 139.
(142) Sabatier, R.; Vasson, A. M.; Vasson, A.; Lethuiller, P.; Soubeyroux, J. L.; Chevalier, R.; Cousseins, J. C. *Mater. Res. Bull.* **1982**, *17*, 369.
(143) Hidaka, M.; Fujii, H.; Garrard, B. J.; Wanklyn, B. M. *Phys. Status Solidi A* **1986**, *95*, 413.
(144) Massa, W.; Steiner, M. *J. Solid State Chem.* **1980**, *32*, 137.
(145) Massa, W. Habilitationsschrift, Marburg, 1982.
(146) Balz, D.; Plieth, K. *Z. Elektrochem.* **1955**, *59*, 545.
(147) Babel, D.; Herdtweck, E. *Z. Anorg. Allg. Chem.* **1982**, *487*, 75.
(148) Kissel, D.; Hoppe, R. *Z. Anorg. Allg. Chem.* **1986**, *541*, 135.
(149) Schnering, H. G. v. *Z. Anorg. Allg. Chem.* **1973**, *400*, 201.
(150) Brosset, C. *Z. Anorg. Allg. Chem.* **1938**, *238*, 201.
(151) Vlasse, M.; Menil, F.; Moriliere, C.; Dance, J. M.; Tressaud, A.; Portier, J. *J. Solid State Chem.* **1976**, *17*, 291.
(152) Jacoboni, C.; Leblê, A.; Rousseau, J. J. *J. Solid State Chem.* **1981**, *36*, 297.
(153) Courbion, G.; DePape, R.; Knoke, G.; Babel, D. *J. Solid State Chem.* **1983**, *49*, 353.
(154) Hidaka, M.; Ono, M. *J. Phys. Soc. Jpn.* **1977**, *43*, 258.
(155) Binder, F. Thesis, Tübingen, 1973.
(156) Haegele, R.; Babel, D. *Z. Anorg. Allg. Chem.* **1974**, *409*, 11.
(157) Hidaka, M.; Hosogi, S. *J. Phys. (Paris)* **1982**, *43*, 1227.
(158) Kijima, N.; Tanaka, K.; Marumo, F. *Acta Crystallogr., Sect. B* **1983**, *B39*, 557.
(159) Miyata, N.; Tanaka, K.; Marume, F. *Acta Crystallogr., Sect. B.* **1983**, *B39*, 561.
(160) Ridou, C.; Rousseau, M.; Pernot, B.; Bouillot, J. *J. Phys. C—Solid State Phys.* **1986**, *19*, 4847.
(161) Okazaki, A.; Suemune, Y. *J. Phys. Soc. Jpn.* **1961**, *16*, 176.
(162) Okazaki, A. *J. Phys. Soc. Jpn.* **1969**, *26*, 870.
(163) Tanaka, K.; Marumo, F. *Acta Crystallogr., Sect. B* **1982**, *B38*, 1422.
(164) Frenzen, G.; Kummer, S.; Massa, W.; Babel, D. *Z. Anorg. Allg. Chem.* **1987**, *553*, 75.
(165) Hardy, A. M.; Hardy, A.; Ferey, G. *Acta Crystallogr., Sect. B* **1973**, *B29*, 1654.
(166) Banks, E.; Nakajima, S.; Williams, G. J. B. *Acta Crystallogr., Sect. B* **1979**, *B35*, 46.
(167) Hartung, A.; Verscharen, W.; Binder, F.; Babel, D. *Z. Anorg. Allg. Chem.* **1979**, *456*, 106.
(168) Masse, R.; Aleonard, S.; Averbuch-Pouchot, M. T. *J. Solid State Chem.* **1984**, *53*, 136.
(169) Leblanc, M.; Ferey, G.; Chevallier, P.; Calage, Y.; DePape, R. *J. Solid State Chem.* **1983**, *47*, 53.
(170) Babel, D. *Z. Anorg. Allg. Chem.* **1972**, *387*, 161.
(171) DePape, R.; Ferey, G. *Mater. Res. Bull.* **1986**, *21*, 971.
(172) Mueller, B. G. *J. Fluorine Chem.* **1981**, *17*, 317.
(173) Ferey, G.; Leblanc, M.; DePape, R. *J. Solid State Chem.* **1981**, *40*, 1.
(174) Wingefeld, G.; Hoppe, R. *Z. Anorg. Allg. Chem.* **1984**, *516*, 223.
(175) Fleischer, T.; Hoppe, R. *J. Fluorine Chem.* **1982**, *19*, 529.
(176) Giuseppetti, G.; Tadini, C. *TMPM, Tschermaks Mineral. Petrogr. Mitt.* **1978**, *25*, 57.
(177) Knop, O.; Cameron, T. S.; Jochem, K. *J. Solid State Chem.* **1982**, *43*, 213.
(178) Haegele, R.; Verscharen, W.; Babel, D.; Dance, J. M.; Tressaud, A. *J. Solid State Chem.* **1978**, *24*, 77.
(179) Kummer, S.; Babel, D. *J. Fluorine Chem.* **1987**, *35*, 157. (a) Kummer, S.; Babel, D. *Z. Naturforsch. B: Anorg. Chem., Org. Chem.* **1987**, *42b*, 1403.
(180) Verscharen, W.; Babel, D. *J. Solid State Chem.* **1978**, *24*, 405.
(181) Hall, W.; Kim, S.; Zubieta, J.; Walton, E. G.; Brown, D. B. *Inorg. Chem.* **1977**, *16*, 1884.
(182) Laligant, Y.; Pannetier, J.; Labbê, P.; Ferey, G. *J. Solid State Chem.* **1986**, *62*, 274.
(183) Laligant, Y.; Calage, Y.; Torres-Tapia, E.; Greneche, J. M.; Varret, F.; Ferey, G. *J. Magn. Magn. Mater.* **1986**, *61*, 283.
(184) Magnéli, A. *Ark. Kemi* **1949**, *1*, 213.
(185) Magnéli, A. *Acta Chem. Scand.* **1953**, *7*, 315.
(186) Poix, P. *C. R. Hebd. Seances Acad. Sci., Ser. C* **1972**, *274*, 620.
(187) Fukunaga, O.; Fujita, T. *J. Solid State Chem.* **1973**, *8*, 331.
(188) Pulcinelli, S. H.; Senegas, J.; Tanguy, B.; Menil, F.; Portier, J. *Rev. Chim. Miner.* **1986**, *23*, 238.
(189) Gaertner, H. R. v. *Neues Jahrb. Mineral., Abh.* **1930**, *61*, 1.
(190) Babel, D.; Binder, F.; Pausewang, G. *Z. Naturforsch., B* **1973**, *28b*, 213.
(191) Hartung, A.; Babel, D. *J. Fluorine Chem.* **1982**, *19*, 369.
(192) Rieck, D.; Langley, R.; Eyring, L. *J. Solid State Chem.* **1982**, *45*, 259.
(193) Schmidt, R. E. Thesis, Marburg, 1985.
(194) Babel, D.; Pausewang, G.; Viebahn, W. *Z. Naturforsch., B* **1967**, *22b*, 1219.
(195) Koch, J.; Hebecker, C. *Naturwissenschaften* **1985**, *72*, 431.
(196) Laligant, Y.; Pannetier, J.; Ferey, G. *J. Solid State Chem.* **1987**, *66*, 242.
(197) Babel, D. *Z. Anorg. Allg. Chem.* **1969**, *369*, 117.
(198) Glazer, A. M. *Acta Crystallogr., Sect. B* **1972**, *B28*, 3384.
(199) Glazer, A. M. *Acta Crystallogr., Sect. A* **1975**, *A31*, 756.
(200) Deblieck, R.; van Tendeloo, G.; van Landuyt, J.; Amelinckx, S. *Acta Crystallogr., Sect. B* **1985**, *B41*, 319.
(201) Massa, W.; Pebler, J. *Studies in Inorganic Chemistry* Elsevier: Amsterdam, 1983; Vol. 3, p 577.
(202) Mueller, B. G. *J. Fluorine Chem.* **1981**, *17*, 409.
(203) Dance, J. M.; Mur, J.; Darriet, J.; Hagenmuller, P.; Massa, W.; Kummer, S.; Babel, D. *J. Solid State Chem.* **1986**, *63*, 446.
(204) Babel, D. *Z. Anorg. Allg. Chem.* **1965**, *336*, 200.
(205) Renaudin, J.; Laligant, Y.; Samouel, M.; DeKozak, A.; Ferey, G. *J. Solid State Chem.* **1986**, *62*, 158.
(206) Holler, H.; Babel, D.; Samouel, M.; DeKozak, A. *Rev. Chim. Miner.* **1984**, *21*, 358.
(207) Holler, H.; Pebler, J.; Babel, D. *Z. Anorg. Allg. Chem.* **1985**, *522*, 189.
(208) Renaudin, J.; Samouel, M.; Leblanc, M.; DeKozak, A.; Ferey, G. *J. Solid State Chem.* **1985**, *59*, 103.
(209) Holler, H.; Babel, D.; Samouel, M.; DeKozak, A. *J. Solid State Chem.* **1981**, *39*, 345.
(210) Renaudin, J.; Calage, Y.; Samouel, M.; DeKozak, A.; Leblanc, M.; Ferey, G. *Rev. Chim. Minerl.* **1985**, *22*, 74.
(211) Holler, H.; Babel, D. *Z. Anorg. Allg. Chem.* **1982**, *491*, 137.
(212) Leblanc, M.; Ferey, G.; DePape, R. *J. Solid State Chem.* **1980**, *33*, 317.
(213) Renaudin, J.; Pannetier, J.; DeKozak, A.; Samouel, M.; Ferey, G. *J. Solid State Chem.* **1986**, *62*, 164.
(214) Viebahn, W. *Z. Anorg. Allg. Chem.* **1975**, *413*, 77.
(215) Courbion, G.; Jacoboni, C.; DePape, R. *Acta Crystallogr., Sect. B* **1977**, *B33*, 1405.
(216) Courbion, G.; Ferey, G.; DePape, R. *Mater. Res. Bull.* **1978**, *13*, 967.
(217) Leblanc, M.; Ferey, G.; Calage, Y.; DePape, R. *J. Solid State Chem.* **1983**, *47*, 24.
(218) Marsh, R. E. *J. Solid State Chem.* **1984**, *51*, 405.
(219) Leblanc, M.; Ferey, G.; DePape, R.; Pannetier, J. *Solid State Commun.* **1986**, *58*, 165.
(220) DeKozak, A.; Samouel, M.; Renaudin, J.; Ferey, G. *Rev. Chim. Miner.* **1986**, *23*, 352.
(221) Renaudin, J.; Ferey, G.; DeKozak, A.; Samouel, M. *Rev. Chim. Miner.* **1986**, *23*, 497.
(222) Steinfink, H.; Burns, J. H. *Acta Crystallogr.* **1964**, *17*, 823.
(223) Rimsky, A.; Thoret, J.; Freundlich, W. *C. R. Hebd. Seances Acad. Sci., Ser. C* **1970**, *270*, 407.
(224) Schmidt, R. E.; Babel, D. *Z. Anorg. Allg. Chem.* **1985**, *529*, 118.
(225) Steinfink, H.; Brunton, G. *Inorg. Chem.* **1969**, *8*, 1665.
(226) Schmidt, R. E.; Babel, D. *Z. Anorg. Allg. Chem.* **1984**, *516*, 187.
(227) Zalkin, A.; Lee, K.; Templeton, D. H. *J. Chem. Phys.* **1962**, *37*, 697.
(228) Dance, J. M.; Grannec, J.; Tressaud, A.; Perrin, M. *Mater. Res. Bull.* **1977**, *12*, 989.
(229) Dance, J. M.; Darriet, J.; Tressaud, A.; Hagenmuller, P. *Z. Anorg. Allg. Chem.* **1984**, *508*, 93.
(230) Krebs, B. *Z. Anorg. Allg. Chem.* **1970**, *378*, 263.
(231) Galasso, F.; Layden, G.; Ganung, G. *Mater. Res. Bull.* **1968**, *3*, 397.
(232) Darriet, J.; Qiang, Y.; Tressaud, A.; Hagenmuller, P. *Mater. Res. Bull.* **1986**, *21*, 1351.
(233) Litvin, A. L.; Petrunina, A. A.; Ostapenko, S. S.; Povarennykh, A. S. *Dopov. Akad. Nauk Ukr. RSR, Ser. B* **1980**, *No. 3*, 47.
(234) Schmidt, R. E.; Pebler, J.; Babel, D. 3rd European Conference on Solid State Chemistry, Regensburg, May 1986.
(235) Hoppe, R. *Adv. Fluorine Chem.* **1970**, *6*, 387.
(236) Pauling, L. *J. Am. Chem. Soc.* **1947**, *69*, 542.
(237) Zachariasen, W. H. *Acta Crystallogr.* **1963**, *16*, 385.
(238) Donnay, G.; Allmann, R. *Am. Mineral.* **1970**, *55*, 1003.
(239) Allmann, R. *Monatsh. Chem.* **1975**, *106*, 779.
(240) Brown, I. D.; Shannon, R. D. *Acta Crystallogr., Sect. A* **1973**, *A29*, 266.
(241) Brown, I. D. *Structure and Bonding in Crystals*; Academic Press: New York, 1981; Vol. II, p 1.
(242) Brown, I. D.; Altermatt, D. *Acta Crystallogr., Sect. B* **1985**, *B41*, 244.
(243) Trömel, M. *Acta Crystallogr., Sect. B* **1983**, *B39*, 664.

(244) Herdtweck, E. Unpublished work, Marburg, 1985.
(245) Welsch, M. Diplomarbeit, Marburg, 1986.
(246) Glemser, O. *J. Fluorine Chem.* **1984**, *24*, 319.
(247) Woolf, A. A. *J. Fluorine Chem.* **1984**, *26*, 481.
(248) Jahn, H. A.; Teller, E. *Proc. R. Soc. London, Sect. A* **1937**, *A161*, 220.
(249) Bersuker, I. B. *The Jahn–Teller Effect and Vibronic Interactions in Modern Chemistry*; Plenum Press: New York, London, 1984.
(250) Reinen, D.; Friebel, C. *Struct. Bonding (Berlin)* **1979**, *37*, 1.
(251) Baur, W. H. *Acta Crystallogr., Sect. B* **1976**, *B32*, 2200.
(252) Bauer, W. H.; Guggenheim, H.; Lin, J.-C. *Acta Crystallogr., Sect. B* **1982**, *B38*, 351.
(253) Baur, W. H.; Khan, A. A. *Acta Crystallogr., Sect. B* **1971**, *B27*, 2133.
(254) Fischer, P.; Hälg, W.; Schwarzenbach, D.; Gamsjäger, H. *J. Phys. Chem. Solids* **1974**, *35*, 1683.
(255) Wieghardt, K.; Weiss, J. *Acta Crystallogr., Sect. B* **1972**, *B28*, 529.
(256) Vedani, A. Thesis, Zürich, 1981.
(257) Knox, K. *Acta Crystallogr.* **1963**, *16*, A45.
(258) Schneider, S.; Hoppe, R. *Z. Anorg. Allg. Chem.* **1970**, *376*, 268.
(259) Massa, W. *Z. Anorg. Allg. Chem.* **1975**, *415*, 254.
(260) Hepworth, M. A.; Jack, K. H. *Acta Crystallogr.* **1957**, *10*, 345.
(261) Herdtweck, E.; Babel, D. *Z. Anorg. Allg. Chem.* **1981**, *474*, 113.
(262) Day, P.; Hutchings, M. T.; Janke, E.; Walker, P. *J. Chem. Soc., Chem. Commun.* **1979**, 711.
(263) Hepworth, M. A.; Peacock, R. D.; Westland, G. L. *Acta Crystallogr.* **1957**, *10*, 63.
(264) Leblanc, M.; Pannetier, J.; Ferey, G.; DePape, R. *Rev. Chim. Miner.* **1985**, *22*, 107.
(265) Crockett, D. S.; Haendler, H. M. *J. Am. Chem. Soc.* **1960**, *82*, 4158.
(266) Morosin, B. *Acta Crystallogr., Sect. B* **1970**, *B26*, 1635.
(267) McDonald, T. R. R. *Acta Crystallogr.* **1960**, *13*, 113.
(268) Massa, W. *Z. Anorg. Allg. Chem.* **1977**, *436*, 29.
(269) Marsh, R. E.; Herbstein, F. H. *Acta Crystallogr., Sect. B* **1983**, *39*, 280.
(270) Decian, A.; Fischer, J.; Weiss, R. *Acta Crystallogr.* **1967**, *22*, 340.
(271) Massa, W. *Z. Anorg. Allg. Chem.* **1976**, *427*, 235.
(272) Epple, M. Thesis, Tübingen, 1978.
(273) Hoppe, R.; Liebe, W.; Dähne, W. *Z. Anorg. Allg. Chem.* **1961**, *307*, 276.
(274) Schlemper, E. V.; Hamilton, W. C. *J. Chem. Phys.* **1966**, *44*, 2499.
(275) Knop, O.; Oxton, I. A.; Westerhaus, W. J.; Falk, M. *Can. J. Chem.* **1979**, *57*, 404. (a) Knop, O.; Oxton, I. A.; Westerhaus, W. J.; Falk, M. *J. Chem. Soc., Faraday Trans. 2* **1981**, *77*, 309.
(276) Moriya, K.; Matsuo, T.; Suga, H.; Seki, S. *Bull. Chem. Soc. Jpn.* **1977**, *50*, 1920.
(277) Knop, O.; Westerhaus, W. J.; Falk, M.; Massa, W. *Can. J. Chem.* **1985**, *63*, 3318.
(278) Lorient, M.; Tressaud, A.; Ravez, J. *Rev. Chim. Miner.* **1980**, *19*, 128.
(279) Pebler, J. *J. Solid State Chem.* **1985**, *56*, 58.
(280) Pebler, J.; Herdtweck, E.; Massa, W.; Schmidt, R. *Studies in Inorganic Chemistry* Elsevier: *Amsterdam*, 1983; Vol. 3, p 501.
(281) Epple, M.; Rüdorff, W.; Massa, W. *Z. Anorg. Allg. Chem.* **1982**, *495*, 200.
(282) Simonov, V. I.; Bukvetsky, B. V. *Acta Crystallogr., Sect. B* **1978**, *B34*, 355.
(283) Prince, E. *J. Chem. Phys.* **1972**, *56*, 4352.
(284) Penfold, B. R.; Taylor, M. R. *Acta Crystallogr.* **1960**, *13*, 953.
(285) Teufer, G. *Acta Crystallogr.* **1964**, *17*, 1480.
(286) Kaučič, V.; Bukovec, P. *J. Chem. Soc., Dalton Trans.* **1979**, 1512.
(287) Fischer, J.; Weiss, R. *Acta Crystallogr., Sect. B* **1973**, *B29*, 1955.
(288) van Ingen Schenau, A. D.; Verschoor, G. C.; de Graaff, R. A. *Acta Crystallogr., Sect. B* **1976**, *B32*, 1127.
(289) Vicat, J.; ThanQui, D.; Filhol, A.; Roudant, E.; Thomas, M.; Aleonard, S. *Acta Crystallogr., Sect. B* **1975**, *B31*, 1895.
(290) Hamilton, W. C. *Acta Crystallogr.* **1962**, *15*, 353.
(291) Clark, M. J. R.; Fleming, J. E.; Lynton, H. *Can. J. Chem.* **1969**, *47*, 3859.
(292) Marseglia, E. A.; Brown, I. D. *Acta Crystallogr., Sect. B* **1973**, *B29*, 1352.
(293) Epple, M.; Massa, W. *Z. Anorg. Allg. Chem.* **1978**, *444*, 47.
(294) Anderson, T. H.; Lingafelter, E. C. *Acta Crystallogr.* **1951**, *4*, 181.
(295) Beursheus, G.; Jeffrey, G. A. *J. Chem. Phys.* **1964**, *41*, 917.
(296) Allmann, R.; Rins, J. *Acta Crystallogr., Sect. A* **1978**, *A34*, 167.
(297) McLean, W. C.; Jeffrey, G. A. *J. Chem. Phys.* **1966**, *44*, 2338.
(298) Mak, T. C. W. *J. Inclus. Phenom.* **1985**, *3*, 347.
(299) Massa, W.; Schmidt, R. E. *Acta Crystallogr., Sect. A* **1984**, *A40*, C-218.
(300) Herdtweck, E. *Z. Anorg. Allg. Chem.* **1983**, *501*, 131.
(301) Sienko, M. J.; Plane, R. A. *Physikalische Anorganische Chemie*; Hirzel: Stuttgart, 1965; p 121.
(302) Mootz, D.; Ohms, U.; Poll, W. *Z. Anorg. Allg. Chem.* **1981**, *479*, 75.
(303) Allen, L. C. *J. Am. Chem. Soc.* **1975**, *97*, 6921.
(304) Carrell, H. C.; Donohue, J. *Isr. J. Chem.* **1972**, *10*, 195.
(305) Massa, W.; Herdtweck, E. *Acta Crystallogr., Sect. C* **1983**, *C39*, 509.
(306) Atoji, M.; Lipscomb, W. *Acta Crystallogr.* **1954**, *7*, 173.
(307) Forrester, J. D.; Senko, M.; Zalkin, A. *Acta Crystallogr.* **1963**, *16*, 58.